



**NAVAL
POSTGRADUATE
SCHOOL**

MONTEREY, CALIFORNIA

THESIS

**INTEGRATION OF COTS UAS WITH MULTISPECTRAL
IMAGING SENSORS TO DETECT CAMOUFLAGED
TARGETS AND BATTLEFIELD ANOMALIES**

by

Stergios Barmpas

June 2023

Thesis Advisor:
Second Reader:

Oleg A. Yakimenko
Fotis A. Papoulias

Approved for public release. Distribution is unlimited.

THIS PAGE INTENTIONALLY LEFT BLANK

REPORT DOCUMENTATION PAGE			<i>Form Approved OMB No. 0704-0188</i>
Public reporting burden for this collection of information is estimated to average 1 hour per response, including the time for reviewing instruction, searching existing data sources, gathering and maintaining the data needed, and completing and reviewing the collection of information. Send comments regarding this burden estimate or any other aspect of this collection of information, including suggestions for reducing this burden, to Washington headquarters Services, Directorate for Information Operations and Reports, 1215 Jefferson Davis Highway, Suite 1204, Arlington, VA 22202-4302, and to the Office of Management and Budget, Paperwork Reduction Project (0704-0188) Washington, DC, 20503.			
1. AGENCY USE ONLY (Leave blank)	2. REPORT DATE June 2023	3. REPORT TYPE AND DATES COVERED Master's thesis	
4. TITLE AND SUBTITLE INTEGRATION OF COTS UAS WITH MULTISPECTRAL IMAGING SENSORS TO DETECT CAMOUFLAGED TARGETS AND BATTLEFIELD ANOMALIES		5. FUNDING NUMBERS	
6. AUTHOR(S) Stergios Barmpas			
7. PERFORMING ORGANIZATION NAME(S) AND ADDRESS(ES) Naval Postgraduate School Monterey, CA 93943-5000		8. PERFORMING ORGANIZATION REPORT NUMBER	
9. SPONSORING / MONITORING AGENCY NAME(S) AND ADDRESS(ES) N/A		10. SPONSORING / MONITORING AGENCY REPORT NUMBER	
11. SUPPLEMENTARY NOTES The views expressed in this thesis are those of the author and do not reflect the official policy or position of the Department of Defense or the U.S. Government.			
12a. DISTRIBUTION / AVAILABILITY STATEMENT Approved for public release. Distribution is unlimited.		12b. DISTRIBUTION CODE A	
13. ABSTRACT (maximum 200 words) In response to the extended use of tactical and theater-level UAS for reconnaissance and surveillance in the modern battlefield, ground forces are increasing their efforts to hide their assets, using camouflage or exploiting terrain and vegetation. In the last decade, the technology of multispectral imaging has evolved, providing compact and low-cost sensors that can enhance the capability of tactical UAS for defeating camouflage and detecting battlefield anomalies that are not visible with EO/IR sensors. In contrast, multispectral sensors provide imaging in multiple narrow bands in the visible and IR spectrum. Computing a difference in absorption and reflectance of different materials in these narrow bands and then fusing these multispectral data in a certain way creates an opportunity to detect even the camouflaged targets. This thesis compares performance of a COTS multispectral imaging sensor integrated with a tactical UAS to detect camouflaged targets and battlefield anomalies against EO/IR sensors. In doing so, it introduces a new image data fusion methodology, examines its effectiveness compared to several other methods, and evaluates its overall performance. The promising results achieved in processing imagery data collected during several field-testing campaigns employing an eVTOL UAS equipped with a MicaSense five-band sensor suggest a necessity to explore this concept further, to include a larger database encapsulating different contemporary camouflage techniques.			
14. SUBJECT TERMS camouflaged target detection, anomaly detection, multispectral imaging, commercial off the shelf, COTS, unmanned aerial systems, UAS		15. NUMBER OF PAGES 103	16. PRICE CODE
17. SECURITY CLASSIFICATION OF REPORT Unclassified	18. SECURITY CLASSIFICATION OF THIS PAGE Unclassified	19. SECURITY CLASSIFICATION OF ABSTRACT Unclassified	20. LIMITATION OF ABSTRACT UU

NSN 7540-01-280-5500

Standard Form 298 (Rev. 2-89)
Prescribed by ANSI Std. Z39-18

THIS PAGE INTENTIONALLY LEFT BLANK

Approved for public release. Distribution is unlimited.

**INTEGRATION OF COTS UAS WITH MULTISPECTRAL IMAGING SENSORS
TO DETECT CAMOUFLAGED TARGETS AND BATTLEFIELD ANOMALIES**

Stergios Barmpas
Captain, Hellenic Army
MSME, National Technical University of Athens, 2018
MS, University of Thessaly, 2021

Submitted in partial fulfillment of the
requirements for the degree of

MASTER OF SCIENCE IN SYSTEMS ENGINEERING

from the

**NAVAL POSTGRADUATE SCHOOL
June 2023**

Approved by: Oleg A. Yakimenko
Advisor

Fotis A. Papoulias
Second Reader

Oleg A. Yakimenko
Chair, Department of Systems Engineering

THIS PAGE INTENTIONALLY LEFT BLANK

ABSTRACT

In response to the extended use of tactical and theater-level UAS for reconnaissance and surveillance in the modern battlefield, ground forces are increasing their efforts to hide their assets, using camouflage or exploiting terrain and vegetation. In the last decade, the technology of multispectral imaging has evolved, providing compact and low-cost sensors that can enhance the capability of tactical UAS for defeating camouflage and detecting battlefield anomalies that are not visible with EO/IR sensors. In contrast, multispectral sensors provide imaging in multiple narrow bands in the visible and IR spectrum. Computing a difference in absorption and reflectance of different materials in these narrow bands and then fusing these multispectral data in a certain way creates an opportunity to detect even the camouflaged targets. This thesis compares performance of a COTS multispectral imaging sensor integrated with a tactical UAS to detect camouflaged targets and battlefield anomalies against EO/IR sensors. In doing so, it introduces a new image data fusion methodology, examines its effectiveness compared to several other methods, and evaluates its overall performance. The promising results achieved in processing imagery data collected during several field-testing campaigns employing an eVTOL UAS equipped with a MicaSense five-band sensor suggest a necessity to explore this concept further, to include a larger database encapsulating different contemporary camouflage techniques.

THIS PAGE INTENTIONALLY LEFT BLANK

TABLE OF CONTENTS

I.	INTRODUCTION.....	1
A.	BACKGROUND	1
	1. Military UAS	1
	2. Military Surveillance and Reconnaissance.....	9
	3. Use of UAS in SR Operations	12
B.	PROBLEM FORMULATION AND THESIS OUTLINE	14
II.	LITERATURE REVIEW	17
A.	AERIAL REMOTE SENSING IMAGING.....	17
	1. EM Radiation Interaction with the Atmospheric and Surface Features.....	17
	2. Visible and IR Imaging Sensors	20
	3. Characterization of Aerial Imaging	22
B.	MULTISPECTRAL IMAGING BASICS, IMPLEMENTATION, AND APPLICATIONS	27
	1. Multispectral Imaging Paradigm	29
	2. Multispectral Imaging Civilian Applications	32
	3. Multispectral Imaging Military Applications	38
III.	EXPERIMENT SETUP.....	41
A.	HARDWARE	41
	1. RedEdge-P Multispectral Sensor.....	41
	2. Trinity F90+ UAS.....	44
B.	AREA OF OPERATIONS	46
C.	DATA COLLECTION PROCEDURE.....	47
IV.	DATA ANALYSIS AND RESULTS	49
A.	SELECTION OF FUSION TECHNIQUES.....	49
B.	POST PROCESS ALGORITHM.....	50
	1. Importing, Aligning, and Cropping Images in MATLAB	51
	2. Arranging Images into a Hypercube.....	54
	3. Generating the Initial Fused Images.....	55
	4. Processing the Initial and Generating the Final Fused Images	57
C.	INTERPRETATION OF THE RESULTS.....	59
	1. Detection of Target in Open Space.....	59

2.	Detection of Target under Partial Vegetation Cover.....	60
3.	Detection of Target under Vegetation Cover	62
4.	Detection of Landmines and IEDs.....	64
V.	CONCLUSIONS AND RECOMMENDATIONS.....	67
A.	CONCLUSIONS	67
B.	LIMITATIONS AND RECOMMENDATIONS FOR FUTURE WORK	68
	APPENDIX. TARGETS CONFIGURATION.....	71
	LIST OF REFERENCES.....	75
	INITIAL DISTRIBUTION LIST	81

LIST OF FIGURES

Figure 1.	Military UAS Mission Growth. Source: Center for Strategic and Budgetary Assessments (2013).....	4
Figure 2.	Alternative UAS Development Paths. Source: Center for Strategic and Budgetary Assessments (2013).....	5
Figure 3.	Unmanned Aircraft Systems Categorization Table. Adapted from Joint Chiefs of Staff (2019).....	6
Figure 4.	Joint UAS Center of Excellence UAS Classification System. Adapted from Office of the Secretary of Defense (2007).....	8
Figure 5.	A Sample of Space-Based Imaging. Source: Wikipedia (n.d.b).....	11
Figure 6.	The MQ-1 Predator Group 4 UAS. Source: Wikipedia (n.d.c).	11
Figure 7.	The RQ-11 Raven Group 1 UAS. Source Wikipedia (n.d.a).....	12
Figure 8.	Synthetic Aperture Radar Imaging. Source: Harney (2013a).....	14
Figure 9.	Spectral Distribution of Energy Radiated from Blackbodies of Various Temperatures. Adapted from Lillesand et al. (2015).	18
Figure 10.	Transmittance of EM Radiation in the IR Part of the Spectrum. Adapted from Harney (2013c).....	19
Figure 11.	Spectral Reflectance of Selected Materials. Source: Jensen (2007).	20
Figure 12.	Monochromatic and Color Image Sensors. Source: Lucid Vision Labs (n.d.).....	22
Figure 13.	Vertical and Oblique Aerial Imaging. Source: Harney (2013b).	23
Figure 14.	The Geometry of a Vertical Aerial Photograph Collected over Flat Terrain. Source: Jensen (2007).	24
Figure 15.	Dependency of Camera Field of View to Camera Lens Angle. Source: Jensen (2007).....	24
Figure 16.	Photographic Coverage along a Flightline. Adapted from Lillesand et al. (2015).	26
Figure 17.	A Block of Aerial Imaging. Adapted from Jensen (2007).....	26

Figure 18.	Spectral Response Curve of a Monochromatic Imaging Sensor. Source: Lucid Vision Labs (2023).....	27
Figure 19.	Spectral Response Curve of a Color Imaging Sensor. Source: Lucid Vision Labs (2023).	28
Figure 20.	Across-Track (a) and Along-Track (b) Multispectral Imaging. Adapted from Jensen (2007).....	30
Figure 21.	Area Arrays for Multispectral Imaging. Adapted from Jensen (2007).....	30
Figure 22.	Typical Vegetation Spectral Reflectance Curve. Source: Jensen (2007).....	33
Figure 23.	Reflectance Response of Leaf as a Function of Water Content. Source: Jensen (2007).....	34
Figure 24.	RGB Imaging of an Agricultural Area.....	36
Figure 25.	CIR Imaging of an Agricultural Area	36
Figure 26.	NIR Band Imaging of an Agricultural Area	37
Figure 27.	RED Band Imaging of an Agricultural Area	37
Figure 28.	NDVI Imaging of an Agricultural Area.....	38
Figure 29.	Camouflage Nets Spectral Reflectance Curve Compared to Vegetation. Source: Shen et al. (2021).	40
Figure 30.	RedEdge-P Multispectral Sensor. Source: AgEagle (n.d.).	42
Figure 31.	RedEdge-P Multispectral Sensor Integrated with UAS. Source: AgEagle (n.d.).....	42
Figure 32.	RedEdge-P Bands. Source: AgEagle (n.d.).	43
Figure 33.	The Trinity F90+ UAS.....	45
Figure 34.	The Trinity F90+ Taking Off.....	46
Figure 35.	The NPS Field Laboratory at McMillan Airfield, Camp Roberts. Source: Google (n.d.).....	47
Figure 36.	Spectral Reflectance Curve of Target and Environment	50
Figure 37.	RedEdge-P Individual Sensors. Adapted from AgEagle (n.d.).	51

Figure 38.	RGB Fusion of Unaligned Multispectral Images.....	52
Figure 39.	Example of Common Features Used in Automatic Image Registration. Source: MathWorks (n.d.).....	53
Figure 40.	RGB Fusion of Aligned, Uncropped Multispectral Images.....	53
Figure 41.	RGB Fusion of Aligned and Cropped Multispectral Images.....	54
Figure 42.	CIR Fusion of Multispectral Images.....	55
Figure 43.	NDVI Fusion of Multispectral Images	56
Figure 44.	NDREB Fusion of Multispectral Images.....	56
Figure 45.	NDVI Fusion of Multispectral Images with Limited Colormap.....	57
Figure 46.	NDREB Fusion of Multispectral Images with Limited Colormap	58
Figure 47.	NDVI Fusion of Multispectral Images with Manual Limited Colormap.....	58
Figure 48.	NDREB Fusion of Multispectral Images with Manual Limited Colormap.....	59
Figure 49.	Imaging of Target in Open Space and without Camouflage, Captured from 100m AGL	60
Figure 50.	Imaging of Target in Open Space and Camouflage, Captured from 100m AGL	60
Figure 51.	Imaging of Target under Partial Vegetation Cover and without Camouflage, Captured from 50m AGL	61
Figure 52.	Imaging of Target under Partial Vegetation Cover and without Camouflage, Captured from 100m AGL	61
Figure 53.	Imaging of Target under Partial Vegetation Cover and Camouflage, Captured from 50m AGL.....	62
Figure 54.	Imaging of Target under Partial Vegetation Cover and Camouflage, Captured from 100m AGL.....	62
Figure 55.	Imaging of Target under Vegetation Cover and without Camouflage, Captured from 50m AGL.....	63
Figure 56.	Imaging of Target under Vegetation Cover and without Camouflage, Captured from 100m AGL.....	63

Figure 57.	Imaging of Target under Vegetation Cover and Camouflage, Captured from 50m AGL.....	64
Figure 58.	Imaging of Target Captured from 50m AGL.....	65
Figure 59.	Imaging of Target Captured from 100m AGL.....	65
Figure 60.	Target at Flight No. 1.....	71
Figure 61.	Target at Flight No. 2.....	71
Figure 62.	Target at Flight No. 3.....	72
Figure 63.	Target at Flight No. 4.....	72
Figure 64.	Target at Flight No. 5.....	73
Figure 65.	Target at Flight No. 6.....	73
Figure 66.	Targets at Flight No. 7.	74

LIST OF TABLES

Table 1.	U.S. Army UAS Echelons	7
Table 2.	RedEdge-P Multispectral Bands. Source: AgEagle (2022).	43
Table 3.	RedEdge-P Sensors Specifications. Source: AgEagle (2022).	44
Table 4.	RedEdge-P General Specifications. Source: AgEagle (2022).	44
Table 5.	Trinity F90+ Specifications. Source: Quantum Systems (n.d.).	45
Table 6.	Experimental Flights Setup.....	48

THIS PAGE INTENTIONALLY LEFT BLANK

LIST OF ACRONYMS AND ABBREVIATIONS

AGL	Above Ground Level
AO	Area of Operations
C4ISR	Command, Control, Communications, Computers, Intelligence, Surveillance, and Reconnaissance
CIR	Color Infrared
COCOMS	Combat Commanders
CONOPS	Concepts of Operations
COTS	Commercial off-the-Shelf
DOD	Department of Defense
EM	Electromagnetic
EO/IR	Electro-Optical/Infrared
IED	Improvised Explosive Device
IR	Infrared
JCS	Joint Chiefs of Staff
LWIR	Long-Wavelength Infrared
MWIR	Mid-Wavelength Infrared
NATO	North Atlantic Treaty Organization
NDREB	Normalized Difference Red Edge Blue
NDVI	Normalized Difference Vegetation Index
NIR	Near-Infrared
NPS	Naval Postgraduate School
SE	Systems Engineering
SR	Surveillance and Reconnaissance

SWIR	Short-Wavelength Infrared
UAS	Unmanned Aerial Systems
VTOL	Vertical Take-off and Landing

EXECUTIVE SUMMARY

This thesis demonstrates the feasibility of using compact, lightweight, and low-cost commercial-off-the-shelf (COTS) multispectral sensors integrated into small tactical unmanned aerial systems (UAS) to enable enhanced detection of camouflaged targets and battlefield anomalies. This capability enhances the detection capabilities of such targets compared to ordinary electro-optical and infrared sensors (EO/IR) used in current designs.

Unmanned systems are used extensively in modern military operations and can provide new or enhanced capabilities and concepts of operation to battlefield commanders and military planners. Their main advantage resides in their ability to perform dull, dirty, and dangerous missions in a more efficient, risk averse, and low-cost manner. For those reasons, unmanned systems, and especially UAS, are nowadays performing most surveillance and reconnaissance operations, providing necessary intelligence at all operational levels.

In response to the extended use of tactical and theater-level UAS for reconnaissance and surveillance in the modern battlefield, ground forces are increasing their efforts to hide their assets, using camouflage, or exploiting terrain and vegetation. Moreover, the widespread use of landmines and improvised explosive devices by regular and irregular forces poses a significant threat to ground forces. Those tactics generate new challenges for intelligence-gathering operations that need to be addressed by new generations of UAS, notably at the tactical level.

In the last decade, the technology of multispectral imaging has evolved, providing compact and low-cost sensors that can enhance the capability of tactical UAS for defeating camouflage and detecting battlefield anomalies that are not visible through regular sensors. In contrast to regular imaging sensors, multispectral devices provide imaging in specific narrow bands in the visible and IR spectrum. In addition, they can enable algorithms that fuse them, aiming to exploit the difference in absorption and reflectance of different materials in those bands.

This research aimed to answer two research questions, calling for the exploration of the capability of COTS multispectral sensors to detect camouflaged man-made targets or battlefield anomalies as well as a comparison of their performance to RGB and panchromatic sensors. To answer those questions, a multispectral sensor integrated into a small tactical-level UAS was used to perform several experimental flights against camouflaged targets. The data collected from those flights was used to evaluate the sensor's performance and explore methods of fusing the multispectral data and generating imaging products.

An algorithm was developed using the MATLAB programming environment to enable the fusion of multispectral data. This algorithm enabled the alignment of the individual multispectral band data and the implementation of three fusion methodologies. The fusion of the multispectral data was performed using the normalized difference vegetation index (NDVI), color infrared (CIR), and the normalized difference red edge blue index (NDREB). NDVI is widely used in commercial agricultural applications to differentiate vegetation and the environment. CIR also highlights vegetation in multicolor imaging. Finally, NDREB was developed for this thesis and exploits the difference in reflectivity between man-made targets and the environment in the red edge and blue bands.

The interpretation of the data collected from the experimental flights proved that COTS multispectral sensors can enable the detection of camouflaged targets and battlefield anomalies and perform better than ordinary EO/IR sensors. Moreover, the performance of the three fusion methodologies that were used was evaluated in several target scenarios. Finally, limitations of the current algorithm for real-time operations were identified. Successfully evaluating a low-cost, compact multispectral sensor in detecting camouflaged targets provided proof of concept for their use in tactical UAS and can be the foundation for future research in this area.

ACKNOWLEDGMENTS

This thesis is not the product of a single individual but a team effort of many, having contributed to it directly or indirectly. Distinguished Professor Oleg Yakimenko and Professor Fotis Papoulias provided me with their undivided support and guidance, and opportunities to explore the examined field further. Without them, this thesis would be poorer in content. Dr. Mike Richardson and the JIFX team provided me with their full support during my participation in JIFX 23–2, in which the experimental flights required for this thesis were conducted. Lieutenant (USCG) Justin Goff was an irreplaceable partner in navigating the strenuous parallel paths of our thesis research.

My deepest gratitude goes to my classmates for their support. From my first day at NPS, feeling like a stranger in a strange land, they accepted me as one of their own and provided me with their full support and cooperation. Furthermore, I would like to thank my Greek compatriots studying at NPS and their families. Without them, living for almost two years away from home would be a far more difficult task. Finally, I am truly grateful to the Hellenic Army and the Technical Corp for providing me the opportunity to study at NPS.

I would like to thank my family, and especially my parents, who raised me and provided me with concrete foundations for every achievement in my life. They are always an inspiration for me through all years of my life. I am thankful to my beloved wife and partner of my life, Anastasia. Without her support and patience, my studies at NPS would be far more challenging.

THIS PAGE INTENTIONALLY LEFT BLANK

I. INTRODUCTION

This chapter will discuss the fundamentals of military unmanned aerial systems (UAS) and their use for conducting surveillance and reconnaissance (SR). At first, the role of UAS in military operations in the past, present, and future is explored, followed by their essential role in SR operations. In the second part of this chapter, and based on this discussion, the problem that this thesis is addressing is formulated.

A. BACKGROUND

1. Military UAS

According to the Department of Defense (DOD), an unmanned system or vehicle is “a powered vehicle that does not carry a human operator, can be operated autonomously or remotely, can be expendable or recoverable, and can carry a lethal or nonlethal payload. Ballistic or semi-ballistic vehicles, cruise missiles, artillery projectiles, torpedoes, mines, satellites, and unattended sensors (with no form of propulsion) are not considered unmanned vehicles” (Office of the Secretary of Defense 2007, 1). Unmanned vehicles are the primary component of unmanned systems in a broader system definition, including ground control stations, remote operators, and communications links. An UAS is a subcategory of unmanned systems, defined as “an aircraft that does not carry a human operator and is capable of flight with or without human remote control, including the necessary equipment, network, and personnel to control the unmanned aircraft” (Joint Chiefs of Staff [JCS] 2010, 252).

Unmanned systems are a crucial part of modern military operations. Started being integrated in mass into military operations since the First Gulf War, their use has increased exponentially since the beginning of the war on terror in the first decades of the 21st century. Every military organization worldwide has recognized the inherited and proven value of their use, as they can enhance current capabilities and enable the development of new concepts of operations (CONOPS).

The reason driving the development and use of unmanned systems in combat operations is their capability to perform more efficiently and risk avert the dull, dirty, dangerous, and covert missions necessary in the modern battlefield (Austin 2010). “Dull” are the missions that require long hours for the operators, creating the conditions for mishaps and low performance. “Dirty” are the missions that require the system to enter a hazardous environment, like an area where chemical warfare agents are present. Finally, “dangerous” are the missions with a high inherent risk, like SR of an area with a high level of enemy threats. Finally, “covert” are the missions where the adversaries shall not be alerted by the platform’s presence. Unmanned systems can perform those missions more cost-effectively without getting the operator in the area of operations (AO).

DOD, in the *Unmanned Systems Roadmap 2007–2032*, identifies key advantages of unmanned platforms connected to the above roles. Those are the capability to provide users regular mission cycles and crew sufficient recovery time, increase the probability of missions meet its objectives, minimizing exposure of operators, and in the case the mission fails to achieve its goal, decrease of human cost and political capital lost. Those advantages are strong motivators for the “continued expansion of unmanned systems across a broad spectrum of warfighting and peacetime operations” (Office of the Secretary of Defense 2007, 19).

In addition to replacing manned platforms in the “dull, dirty, or dangerous” missions (Austin 2010, 5), CONOPS have emerged that utilize UAS in new and novel ways. In a report to Congress, the Congressional Research Service identifies aircraft system-of-systems, artificial intelligence-enabled manned-unmanned teaming, swarming, and lethal autonomous systems as future and experimental concepts in the field (Hoehn, Sayler, and DeVine 2022). Those concepts have the potential to revolutionize warfare in the near future. However, they are also creating issues, from legal and ethical concerns to the enhancement of cyber vulnerabilities and the need for trust-building between soldiers and machines. Nevertheless, the benefits outmatch the drawbacks. Military organizations need to adapt and evolve into an autonomous-centric future to remain relevant and keep the competitive advantage compared to their adversaries.

a. Past, Present and Future of Military UAS

Unmanned platforms have been developed and used since the interwar era. Nevertheless, military UAS before the First Gulf War tended to provide limited, niche capabilities designed to address specific operational problems (Center for Strategic and Budgetary Assessments 2013). The modern military UAS as we know it today was a product of the U.S. Joint Program Office and the Defense Airborne Reconnaissance Office taking overall research, development, and procurement of UASs for each service (Blom 2010). The most successful program emerging from this effort was the medium-range MQ-1 “Predator,” which, together with the Defense Advanced Research Projects Agency–United States Air Force-developed RQ-4 “Global Hawk” defined the use of UAS in SR operations during the first decade of the 21st century and the global war on terror.

Figure 1 highlights the historical evolution of UAS, from the aerial torpedoes and target drones to the modern high altitude long endurance UAS that patrol the skies worldwide. Nowadays, UAS are performing a wide range of missions, from force protection to anti-submarine operations and command and control. In 2006, combat commanders (COCOM) identified reconnaissance and precision target location and designations as the first and second most important missions that the DOD should focus on developing new UAS (Office of the Secretary of Defense 2007). Based on the COCOMs and military department needs, the Unmanned Systems Roadmap for 2007–2032 identifies reconnaissance, target identification and designation, counter-mine warfare, and chemical, biological, radiological, nuclear, and explosive reconnaissance as its main priorities in UAS development and fielding (Office of the Secretary of Defense 2007).

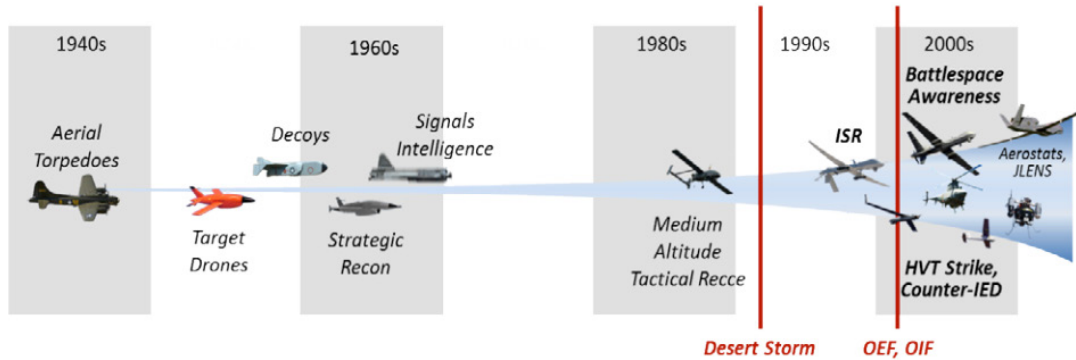


Figure 1. Military UAS Mission Growth. Source: Center for Strategic and Budgetary Assessments (2013).

UAS are already playing a significant role in modern operations, providing COCOMs with new capabilities to support their mission and planning and retain and sustain enhanced situational awareness. Nevertheless, twenty years of fighting the war on terror and small wars worldwide created a persistent focus on current operations, optimizing current capabilities and CONOPS (Center for Strategic and Budgetary Assessments 2013). While restructuring and retraining the armed forces for future challenges, the DOD needs to create a new vision for the development and use of UAS in near-future operations.

The Center for Strategic and Budgetary Assessments (2013) proposed a three-pronged approach to alternative UAS development paths, presented in Figure 2. The first alternative path calls for optimizing the current UAS force for use in permissive environments and support roles. A new path for multi-mission, autonomous, long endurance, and low observability UAS must be pursued to penetrate high-threat environments supporting conventional forces or autonomous modes. Finally, to support high-tempo operations against competent adversaries, small, cheap, expendable, and swarming UAS can be used to conduct high-risk and anti-access and area denial operations.

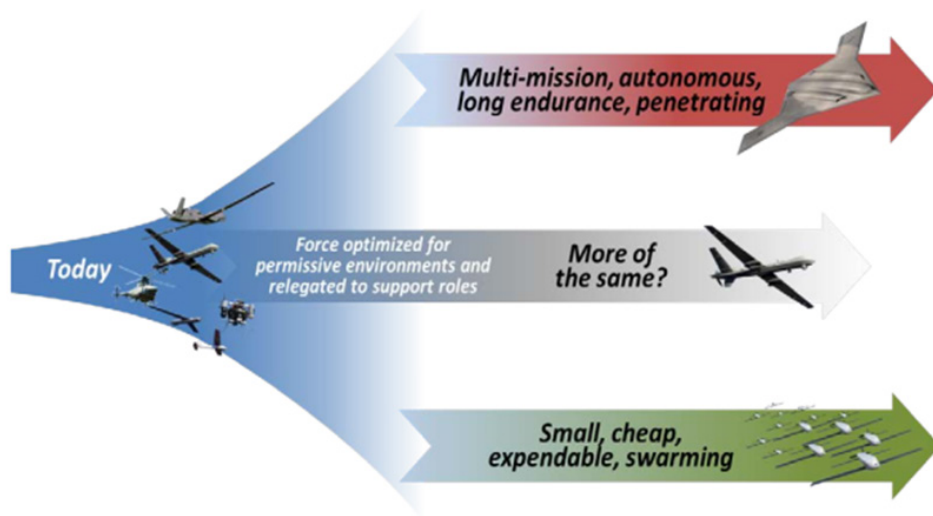


Figure 2. Alternative UAS Development Paths. Source: Center for Strategic and Budgetary Assessments (2013).

To address the challenges of the development of future UAS, capable of addressing the challenges of the multi-domain modern battlefield, DOD recognizes the need to focus on four critical themes, which will “address foundational areas of interest that will continue to accelerate unmanned systems into the future” (Office of the Assistant Secretary of Defense for Acquisition 2017, v). According to the Office of the Assistant Secretary of Defense for Acquisition, those areas of interest are:

- interoperability, including common/open architectures, modularity, and parts interchangeability,
- autonomy, including artificial intelligence and machine learning, increased efficiency, effectiveness, trust, and weaponization,
- network security, including cyber operations, information assurance, and electromagnetic and electronic warfare, and
- human-machine collaboration, including interfaces and teaming. (Office of the Assistant Secretary of Defense for Acquisition 2017, 4–5)

b. Classification of Military UAS

UAS are classified based on performance characteristics or operational utilization. DOD classifies UAS into five groups based on a combination of the following parameters, as presented in Figure 3:

- Maximum gross take-off weight
- Normal operating altitude
- Speed

UA Category	Maximum Gross Takeoff Weight (lbs)	Normal Operating Altitude (ft)	Speed (KIAS)	Representative UAS
Group 1	0-20	< 1200 AGL	100 kts	WASP III, TACMAV RQ-14A/B, Buster, Nighthawk, RQ-11B, FPASS, RQ16A, Pointer, Aqua/Terra Puma
Group 2	21-55	< 3500 AGL	< 250	ScanEagle, Silver Fox, Aerosonde
Group 3	< 1320	< 18,000 MSL	< 250	RQ-7B Shadow, RQ-15 Neptune, XPV-1 Tern, XPV-2 Mako
Group 4	> 1320		Any Airspeed	MQ-5B Hunter, MQ-8B Fire Scout, MQ-1C Gray Eagle, MQ-1A/B/C Predator
Group 5	> 1320	> 18,000 MSL	Any Airspeed	MQ-9 Reaper, RQ-4 Global Hawk, RQ-4N Triton

Figure 3. Unmanned Aircraft Systems Categorization Table. Adapted from Joint Chiefs of Staff (2019).

The U.S. Army utilizes the current classification systems, but to integrate UAS operations more efficiently into the current structure and concepts of operations (CONOPS) has developed a three-tier UAS echelon system, presented in Table 1 (U.S. Army UAS Center of Excellence 2010). Moreover, for connecting UAS groups with COCOMS levels, DOD classifies Group 1 and 2 UAS as Small, Group 3 as Tactical, and Group 5 as Theater level, identifying the subcategory of Combat UAS (Office of the Secretary of Defense 2007). Finally, the Joint UAS Center of Excellence has introduced an attributed-based classification system presented in Figure 4. Combined with the capability needs and CONOPS, these supplementary systems enable designers to tailor UAS

requirements more efficiently than utilizing only the group classification system; nevertheless, the need for a new classification system is evident.

Table 1. U.S. Army UAS Echelons

Echelon	Range (km)	Mission Duration (hr)	Integration Level
Battalion	<25	1–2	Integrated into the scheme of the maneuver as an organic asset supporting operations
Brigade	<125	5–10	Fully integrated with ground forces and other aviation assets characterize UAS operations at the area.
Division and higher	>200	>16	Fully integrated with ground forces and other aviation assets characterize UAS operations at the area.

JUAS Categories	Current System Attributes						
	Operational Altitude (ft)	Typical Payload	Launch Method	Weight (lbs)	Airspeed (kts)	Endurance (hrs)	Radius (nm)
T1 - Tactical 1 Special Operations Forces (SOF) Team Small Unit Company & below	≤ 1,000	Primarily EO/IR or Comm Relay	Hand launched	≤ 20	≤ 60	< 4	< 10
T2 - Tactical 2 Battalion/Brigade Regiment SOF Group/Flight	≤ 5,000		Mobile launched	20 - 450	≤ 100	< 24	< 100
T3 - Tactical 3 Division/Corps MEF/Squadron/Strike Group	≤ 10,000	Above, plus SAR, SIGINT, Moving Target Indicator (MTI), or WPNS	Conventional or Vertical Take-off and Landing (VTOL)	450 – 5,000	≤ 250	< 36	< 2,000
O - Operational JTF	≤ 40,000		Conventional	≤ 15,000	> 250		
S - Strategic National	> 40,000		Above, plus RADAR	> 15,000			

Figure 4. Joint UAS Center of Excellence UAS Classification System. Adapted from Office of the Secretary of Defense (2007).

The inability of the Group classification system to consider parameters like the operational level, mission type, mode of operation, cost, endurance, sensor package, and the several parallel classification systems used by institutions inside the DOD generates difficulties for requirements generation and acquisitions. This difficulty led Congress to introduce Unmanned Aircraft Systems Review Act of 2021 (H.R. 6245, 117th Cong.) that requires a review of the current classification system based on the following parameters:

1. The future capability and employment needs to support current and emerging warfighting concepts;
2. Advanced systems and technologies available in the current commercial marketplace;
3. The rapid fielding of unmanned aircraft systems technology; and
4. The integration of unmanned aircraft systems into the National Airspace System. (Sec. 2).

2. Military Surveillance and Reconnaissance

Two essential elements of modern warfare are SR. They are elements of the command, control, communications, computers, intelligence, surveillance, and reconnaissance (C4ISR) concept, and they build the foundation for all military operations by providing “better situational awareness of the conditions on the ground, in the air, at sea, in space and in the cyber domain” (NATO 2023). The primary objectives of SR are gathering intelligence, monitoring, and tracking enemy movements, and providing a tactical advantage in military operations. Several definitions of SR exist; nevertheless, their main elements remain the same regardless of the organization using them.

Two of the largest military organizations defining SR are the DOD and the North Atlantic Treaty Organization (NATO). According to the U.S. Armed Forces, surveillance is “the systematic observation of aerospace, surface, or subsurface areas, places, persons, or things, by visual, aural, electronic, photographic, or other means” and reconnaissance “a mission undertaken to obtain, by visual observation or other detection methods, information about the activities and resources of an enemy or adversary, or to secure data concerning the meteorological, hydrographic, or geographic characteristics of a particular area” (JCS 2022, GL-10). NATO defines surveillance as “the persistent monitoring of a target” and reconnaissance as “information-gathering conducted to answer a specific military question” (NATO 2023). Although surveillance and reconnaissance are methods for gathering information about enemy activity, their definitions highlight their scope, timing, and purpose differences.

Surveillance is an ongoing monitoring activity performed for extended periods. It usually covers a broader area or target, with the scope of detecting changes in the enemy’s behavior, activities, or characteristics and the environment. Depending on its purpose,

surveillance can be defined as strategic or local/tactical. Strategic surveillance aims at large areas, with some targets being existing infrastructure and expansion efforts, land use, or large-scale order of battle. Local surveillance monitors specific, confined areas and targets and tracks any ongoing changes, movements, or activities, even while an operation is ongoing (Harney 2013b). Both strategic and tactical surveillance use the same intelligence-gathering methods, with the difference in the scale and size of the platform involved.

In contrast to surveillance, reconnaissance involves a single set of observations on a limited area or target (Harney 2013b). It is usually conducted before an operation to gather intelligence about the enemy's location, strength, and intentions. Its scope is to support informed decisions about tactics, strategy, and logistics. Reconnaissance's main difference from surveillance is its duration (Harney 2013b). According to NATO, "Surveillance is a more prolonged and deliberate activity, while reconnaissance missions are generally rapid and targeted to retrieve specific information" (NATO 2013).

The methods of conducting SR are usually classified based on the domain where the SR platform/sensor operates. Based on the most common SR methods are the following (Harney 2013b):

- Surface-based SR: When the platform/sensor used is operating on the surface of the Earth, then it is classified as a surface method for conducting SR. A sub-classification of those methods is the distinction between sea-surface based and earth-surface based methods, with sub-surface being a sub-classification of sea-surface.
- Space-based SR: When the platform/sensor operates in space (higher than the threshold of the Karman line - 100 km), it is classified as a space-based method for conducting SR. One example of such a method is "spy" satellites built for remote sensing and imaging of targets on the planet's surface. Figure 5 provides an example showing "an image (resolution 10 cm/px) of the damaged launch pad at Imam Khomeini Spaceport at Iran, after a rocket explosion on 29 August 2019, speculated as being taken by a KH-1" (Wikipedia, n.d.b).

- Airborne-based SR: When the platform/sensor operates inside the Earth's atmosphere, under the Karman line and above the surface, it is classified as an airborne-base method of conducting SR. Airborne-based methods can use fixed wing airplanes, rotorcrafts, balloons, and other platforms, manned and unmanned (Figures 6 and 7).



Figure 5. A Sample of Space-Based Imaging. Source: Wikipedia (n.d.b).



Figure 6. The MQ-1 Predator Group 4 UAS. Source: Wikipedia (n.d.c).



Figure 7. The RQ-11 Raven Group 1 UAS. Source Wikipedia (n.d.a).

3. Use of UAS in SR Operations

Over the past 20 years, the U.S. Armed Forces have used UAS as the primary method for information gathering and execution of SR operations (Harbaugh 2018). UAS has emerged as one of the most prominent airborne-based methods of conducting SR operations on the modern battlefield. They are the descendent of observation balloons, photo planes, and dedicated “spy” airplanes like the Lockheed Martin’s U2 and SR-71. Nowadays, numerous UAS are operating in all services around the world, conducting SR operations over every type of area of operation.

U.S. Army in its UAS roadmap, describes the use of UAS in SR operations as “the ability to collect current data on enemy terrain, organization, and infrastructure and also to support adaptive, real-time planning, including monitoring enemy centers of gravity, capabilities, and offensive and defensive positions, as well as assessing battle damage after the fact” (U.S. Army 2010, 17). According to Glade (2010), the main advantages of the use of UAS for SR operations compared to manned platforms are:

- They can work faster, more precisely, and reliably than human operators.
- They have higher endurance and loiter time.
- They can operate in or near high-threat or hazardous environments.

- They can be less susceptible and vulnerable to enemy threats.

Similarly, the Defense Science Board identifies the following factors under which UAS can benefit DOD missions. Those factors are the main elements of most SR missions and the operations they support; thus, they make evident the reasons behind the exponential increase in the use of UAS in SR missions (Harbaugh 2018):

- Rapid decision-making.
- High heterogeneity and/or volume of data.
- Intermittent communications.
- High complexity of coordinated action.
- Danger of mission.
- High persistence or endurance (Defense Science Board 2016, iii).

Sensor payloads enable UAS to perform SR missions, with their cost representing as high as half the cost of the whole platform (Office of the Secretary of Defense 2005). The primary data collection technologies in UAS are imaging sensors (Harbaugh 2018), with signal intelligence arrays also providing significant capabilities. The most common imaging sensors in use with UAS are electro-optical/infrared (EO/IR) and synthetic aperture radar, with LIDAR and multispectral/hyperspectral being prominent emerging technologies already used in several civilian applications and high-tier military UAS.

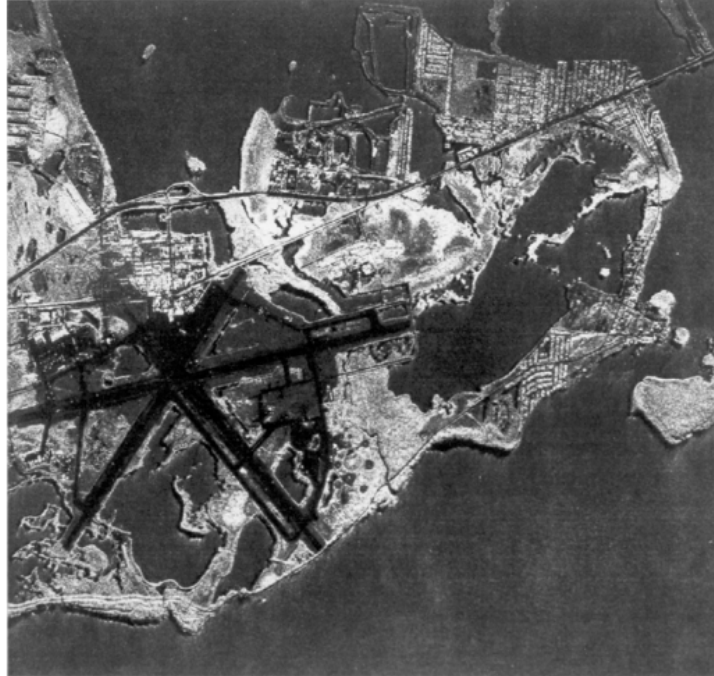


Figure 8. Synthetic Aperture Radar Imaging. Source: Harney (2013a).

B. PROBLEM FORMULATION AND THESIS OUTLINE

The Defense Science Board, in their summer study on autonomy (Defense Science Board 2016), identifies the need for organic tactical UAS to support ground forces in their operations and recognizes that existing platforms, like the RQ-11 Raven, are not capable of supporting the rapidly evolving needs of an agile force. Moreover, the EO/IR sensors integrated into the current generation of tactical UAS provide good day and night imaging; nevertheless, using camouflage and vegetation to achieve cover can achieve the necessary deception for the target not to be detected.

Based on this analysis, tactical ground forces at the battalion level and below do not possess the capability to perform SR operations capable of detecting effectively camouflaged and hidden targets as well as landmines and IEDs. This capability gap generates the need for a UAS SR system, highly mobile, range adequate for tactical operations, easy to operate, has a quick deployment timeframe, and is capable of detecting camouflaged and covered targets.

This need generates the following high-level requirements for the UAS SR system:

- Deployable by soldiers in a timeframe that meets the operational tempo of tactical operations.
- Deployable without the need for special equipment.
- Range equal to or higher to the maximum range of a battalion's intelligence area of interest.
- Autonomous or semi-autonomous operation.
- Sensors that can defeat camouflage and vegetation or other cover.
- Low acquisition and operational cost

To meet those requirements, the UAS SR systems under examination shall at least incorporate the following characteristics:

- Deployment method that does not require a runway or specialized vehicles or equipment like take-off ramps.
- Mission software and flight controller capable of preprogrammed or assisted autonomous or semi-autonomous flight.
- Sensors that can provide enhanced performance from current EO/IR systems.
- Low-cost design

A full exploration of the design space leading to solutions for designing a system capable of meeting those requirements and features would have to reach for new technologies and solutions currently used in higher-level systems. Moreover, evaluating compact and low-cost commercial-off-the-shelf (COTS) components providing new capabilities at a lower cost can be critical to achieving the requirement for system affordability. This thesis aims to support the development effort for low-cost and highly

capable tactical UAS by examining COTS multispectral sensors' performance in detecting camouflaged targets and battlefield anomalies.

Office of the Secretary of Defense (2005) identifies that multispectral imaging combined with the attributes of panchromatic sensors can create fused images that can provide valuable information about enemy targets and excellent counter to common camouflage concealment and denial tactics used by adversaries. To evaluate the performance of multispectral sensors, this thesis strives to answer two critical research questions:

1. Are commercial-off-the-shelf (COTS) multispectral sensors integrated with a UAS capable of detecting camouflaged man-made targets or battlefield anomalies?
2. Do COTS multispectral sensors provide a better detection capability than RGB and panchromatic sensors?

This thesis examined the capability of an integrated into a small UAS, COTS multispectral sensor designed for use in several civilian applications, like agriculture and topography, to capture imaging of camouflaged targets and battlefield anomalies and how the imaging products compare to ordinary EO/IR imaging sensors. The thesis is organized as follows:

- Chapter II discusses multispectral/hyperspectral imaging technology and how it can be used to support the detection of camouflaged targets and battlefield anomalies.
- Chapter III presents the experimental design for the flights conducted supporting data collection.
- Chapter IV discusses the collected data's processing and evaluation.
- Chapter V summarizes the thesis with conclusions and recommendations for future work.

II. LITERATURE REVIEW

In this chapter we review literature on the related technologies and approaches concerning multispectral imaging and the use of such sensors in civilian and military applications. We start with discussing the basics of aerial remote sensing and then proceed with discussing the technology of multispectral imaging followed by its civilian and military applications.

A. AERIAL REMOTE SENSING IMAGING

According to Schott, “the broad definition of remote sensing would encompass vision, astronomy, space probes, most medical imaging, nondestructive testing, sonar, observing the earth from a distance, and many other areas” (Schott 2007, 1) This definition includes every capability that provides information for an object or phenomenon gathered remotely. This thesis will restrict this definition to earth observation from above its surface, exploiting the electromagnetic (EM) spectrum. Moreover, from the full spectrum of capabilities under the term remote sensing, we will examine imaging, being defined as the process of creating visual representations of objects, structures, or phenomena using the visible and infrared (IR) part of the EM spectrum. From this definition, imaging products created by synthetic aperture radars are excluded for the purposes of this thesis. Restricted to this context, imaging is one of the main capabilities enabling RS operations, as described in the previous chapter.

1. EM Radiation Interaction with the Atmospheric and Surface Features

The EM spectrum is broad, and almost every part of it is exploited by humans, enabling numerous technologies. Even so, humans can only sense with their “optical sensors,” just a small part of it, limited to the so-called “visible” part of the EM spectrum, ranging from 380 nm to 750 nm. For imaging purposes, other parts of the EM spectrum can also provide information that contributes to the creation of better representations of the environment and objects in it. The IR part of the EM spectrum is the most widely used for this purpose, residing at wavelengths from 750nm to 1mm.

The IR part of the spectrum can enable the imaging of objects even when no visible light source is present due to the wavelength of radiation emitted by objects with temperatures under 1000K being in the IR spectrum range. This is presented in Figure 9, depicting the black body radiation curve for various temperatures. Atmospheric attenuation of EM radiation in the IR part of the spectrum imposes barriers on the exploitation of the whole IR spectrum, creating specific windows where useful imaging can be conducted. Those windows define the sub-division of the IR radiation in the following categories (Harney 2013c), presented in Figure 10:

- Near-infrared (NIR), from 0.75 to 1.4 μm .
- Short-wavelength infrared (SWIR), from 1.4 to 3 μm .
- Mid-wavelength infrared (MWIR), from 3 to 8 μm .
- Long-wavelength infrared (LWIR), from 8 to 15 μm .

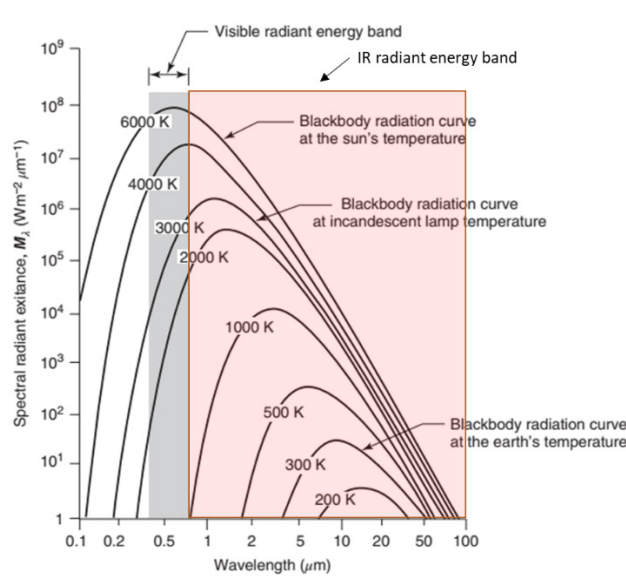


Figure 9. Spectral Distribution of Energy Radiated from Blackbodies of Various Temperatures. Adapted from Lillesand et al. (2015).

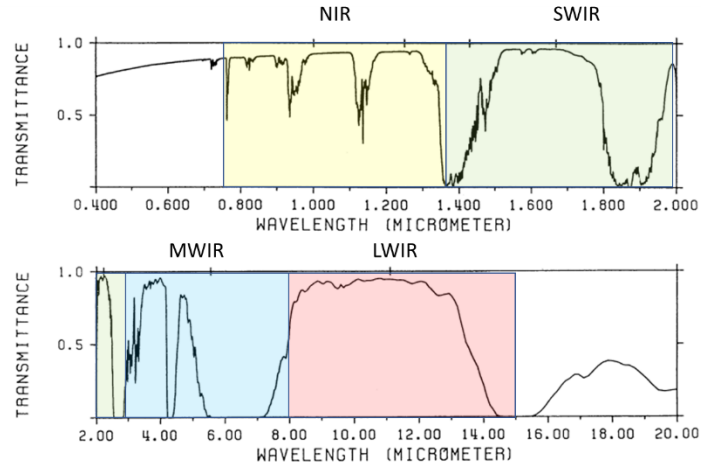


Figure 10. Transmittance of EM Radiation in the IR Part of the Spectrum.
Adapted from Harney (2013c).

EM radiation from the sun or created by other sources propagates in the atmosphere, affected by scattering and absorption until it is incident on any given earth’s surface features. The incident energy can be reflected, absorbed, and/or passed the surface. By using the principle of conservation of energy, this interaction can be expressed as

$$E_I(\lambda) = E_R(\lambda) + E_A(\lambda) + E_T(\lambda), \quad (1)$$

where E_I , E_R , E_A , and E_T , are the incident, reflected, absorbed, and transmitted energy respectfully as a function of wavelength (λ) (Lillesand et al. 2015).

Equation 1 expresses energy conservation, indicating that the reflected energy is equal to the incident energy minus the energy absorbed or transmitted through the new medium. Each surface reflects, absorbs, or transmits EM radiation differently, depending on the surface’s medium’s material and the incident radiation’s wavelength. This property of each surface is called spectral reflectance, it is a function of wavelength and expresses the percentage of the incident radiation that was reflected. Equation (2) expresses this property as a percentage (Lillesand et al. 2015).

$$\rho_\lambda = \frac{E_R(\lambda)}{E_I(\lambda)} \times 100 \quad (2)$$

Equations (1) and (2) indicate that each material has a different spectral reflectance along the EM spectrum. The graph that visualizes this property of materials is called a spectral reflectance curve. Figure 11 compiles several spectral reflectance curves in the visible and IR part of the EM spectrum. Along with the transmittance of EM radiation, spectral reflectance curves can influence the design of systems and algorithms for imaging and remote sensing in general.

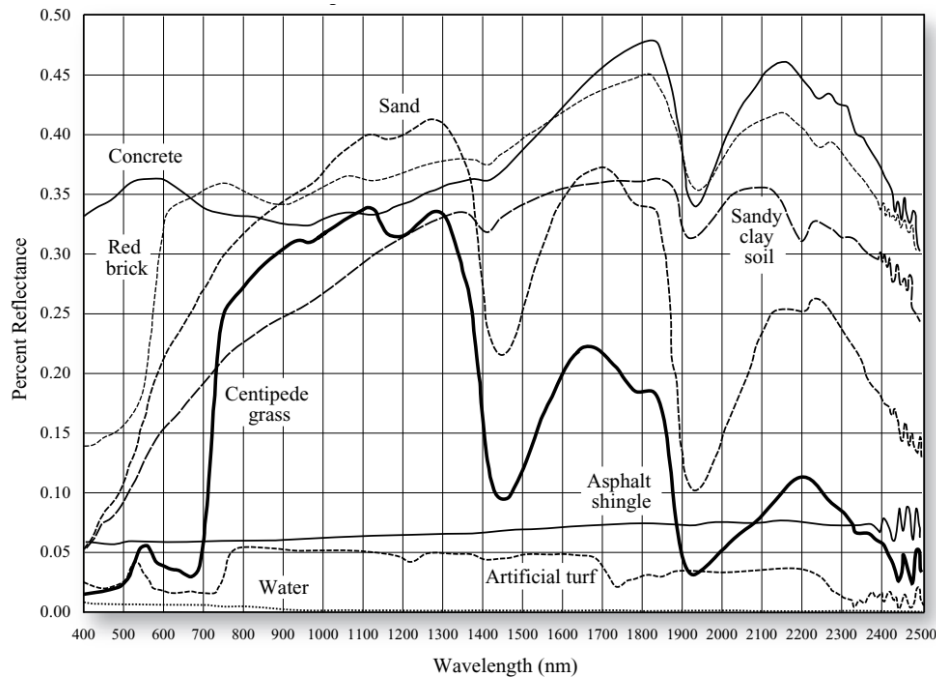


Figure 11. Spectral Reflectance of Selected Materials. Source: Jensen (2007).

2. Visible and IR Imaging Sensors

For the longest period of aerial imaging, photographic film was the medium in which information was captured and recorded (Harney 2013b). The photographic film offered excellent quality and resolution but came with several disadvantages. The more serious ones were the finite number of images it could store and the need to be delivered to the ground and developed before any images could be exploited. Nowadays, digital image sensors have replaced films almost in every application. They provide high resolution and the capability to store a significantly higher number of images that can also

directly transfer to a ground station using a datalink of adequate bandwidth, even as a live feed video. Digital imaging sensors in the optical and infrared part of the EM spectrum are usually called electro-optical and infrared sensors.

Digital visible image sensors consist of numerous photodiodes called pixels. Pixels work as quantum detectors that can respond to individual photons and create an electrical signal analogous to the energy of the incident photons (Harney 2013a). A digital image sensor is an array of pixels that can create monochromatic or color images. In both cases, the image created is a wideband depiction of the incoming EM radiation in the visible part of the spectrum. To create color images, pixels are covered with wideband filters for red, green, and blue parts of the visible part of the spectrum and combine their signals to create an RGB image. Figure 12 presents an example of a monochromatic and color imaging sensor. Several IR sensors work in the same way as visible imaging sensors, with their photodiodes calibrated to react to photons on the IR part of the spectrum. In contrast, others use thermal electromotive force detectors that exploit the temperature change to create a corresponding current or voltage change (Harney 2013a).

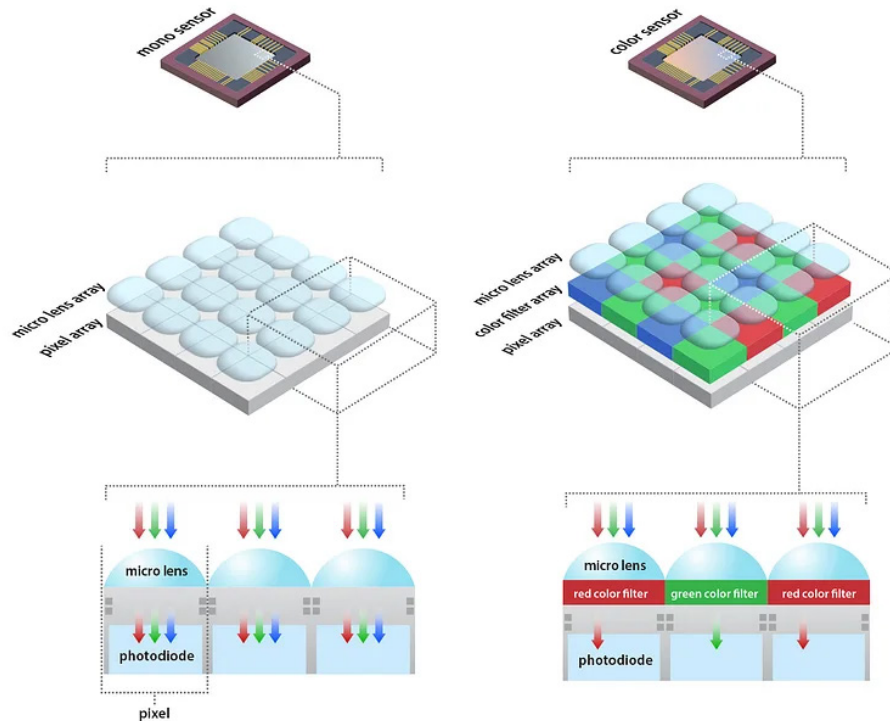


Figure 12. Monochromatic and Color Image Sensors. Source: Lucid Vision Labs (n.d.).

Each sensor is enclosed in a camera body, including a lens, a shutter, and the required control electronics. The main characteristics of cameras are the focal length, f /stop, and shutter speed. The focal length is defined as “the distance from the rear nodal point of the lens to the sensor plane” (Jensen 2009, 69). In general, when the height the platform using the sensor is flying, the higher the focal length must be to produce detailed imaging. f /stop and shutter speed control the amount of light that reaches the sensor, thus controlling the image’s brightness. The range and/or values of the abovementioned characteristics design parameters are directly affected by the mission profile in which the sensor will be used.

3. Characterization of Aerial Imaging

Aerial imaging uses EO/IR sensors mounted to aerial platforms, aiming to obtain images or video of areas under and/or on the sides of the platform. The two typical modes of operation for aerial imaging using EO/IR sensors are vertical and oblique. Vertical

imagers aim straight down at a 90° depression angle for the horizontal axis, and can provide data like what is displayed on a map. Using vertical images, determining horizontal dimensions and distance can be an easy task. On the other hand, depth determination cannot be accurately estimated. Oblique imaging is taken from the side, with depression angles varying between 5° and 60° . In contrast to vertical imaging, oblique imaging can provide data for estimating the depth/height of objects but not for accurate estimations of horizontal dimensions (Harney 2013b). Figure 13 provides a clear representation of vertical and oblique imagery.

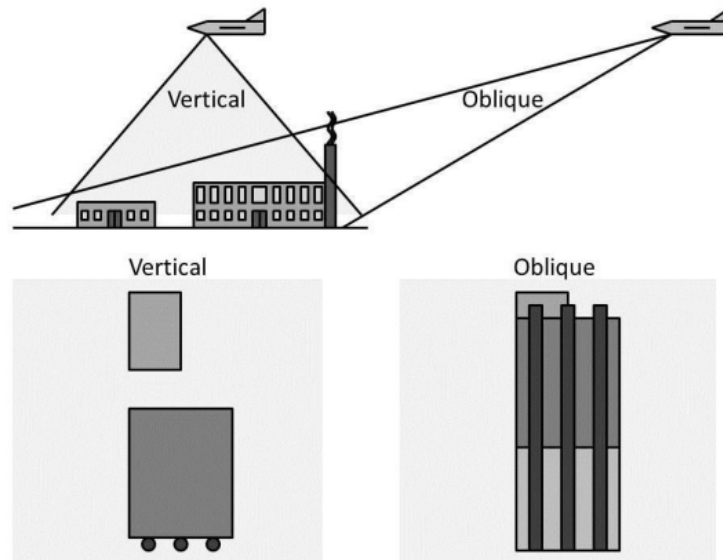


Figure 13. Vertical and Oblique Aerial Imaging. Source: Harney (2013b).

The surface area covered by the imagery taken by the sensor depends on various factors. Figure 14 presents the geometry of vertical aerial imaging over relatively flat terrain. We observe that the surface area that can be represented in the positive print area depends on the focal length, the altitude of the platform, as well as the angle of the lens. Figure 15 presents how greater lens angles can provide a greater camera field of views and imagery of larger areas.

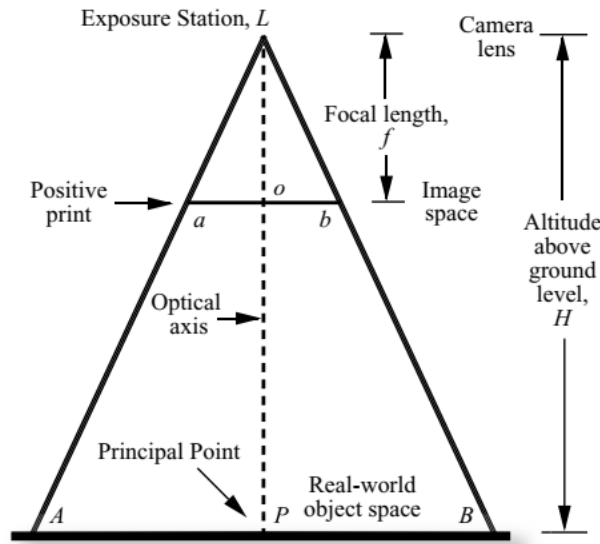


Figure 14. The Geometry of a Vertical Aerial Photograph Collected over Flat Terrain. Source: Jensen (2007).

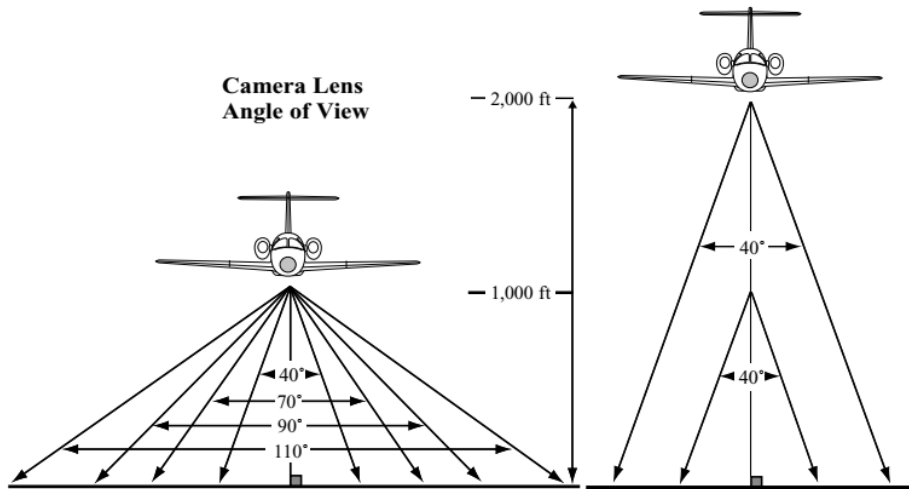


Figure 15. Dependency of Camera Field of View to Camera Lens Angle. Source: Jensen (2007).

To provide imaging for a successful SR, a large area must be captured in many individual images that can be combined to create a better representation of the area. For this to be achieved, the platform in which the sensor is mounted performs a flightline. During this movement, it captures images in a specific timeline, depending on the speed of

the aerial platform and the scale of the desired photography (Jensen 2007). Usually, the images captured are linearly overlapped by a specific percentage and have a sidelap between different sections of the flightline, enabling a more straightforward combination of the captured images. The concept of the flightline, overlaps, and sidelaps is presented in Figures 16 and 17.

The main trade-off faced by designers and operators of aerial imaging systems is the one between coverage and resolution. Digital cameras have a finite number of pixels in both vertical and horizontal dimensions. The linear coverage (X) of a sensor depends on the number of pixels in this dimension (N) and the spatial resolution measuring the smallest object that can be resolved by the sensor (x), or the angular size of the image (θ) and the angular resolution of the sensor (α) (Harney 2013b). This dependence is expressed by Equation 3.

$$N = X / x = \theta / \alpha \quad (3)$$

Spatial resolution is a critical requirement for object detection. The target size shall be larger than the spatial resolution of the imaging sensor for the imaging product to represent the target as at least one pixel, enabling its distinction from the environment. On the other hand, if the spatial resolution is larger than the target size, then the target signal is mixed with the background, entering the subpixel detection regime (Skauli and Kasen 2005). When designing or selecting a sensor, identifying potential targets, and selecting a spatial resolution at least equal to the smallest of them must be considered a critical requirement.

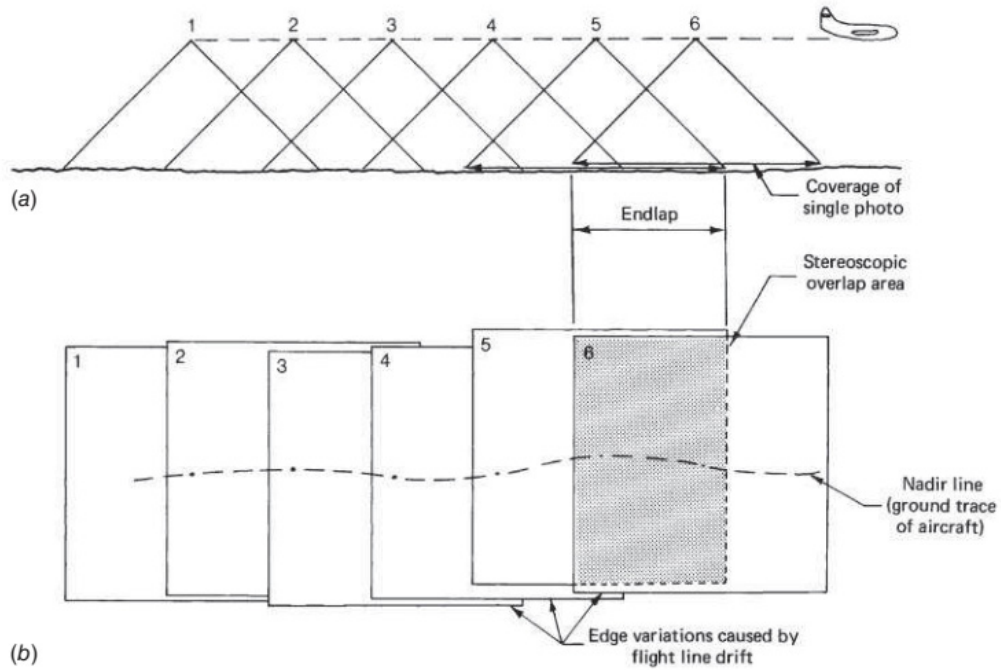


Figure 16. Photographic Coverage along a Flightline. Adapted from Lillesand et al. (2015).

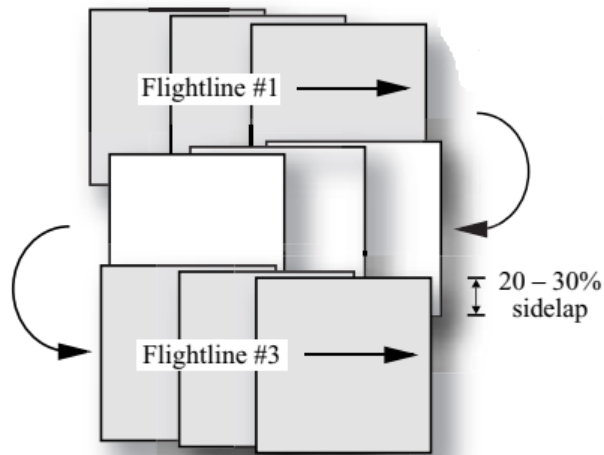


Figure 17. A Block of Aerial Imaging. Adapted from Jensen (2007).

B. MULTISPECTRAL IMAGING BASICS, IMPLEMENTATION, AND APPLICATIONS

Ordinary EO/IR sensors capture data from a single and wide part of the EM spectrum or from a limited number of broad wavebands. Monochromatic sensors use a single full visible spectrum band, while color sensors use red, green, and blue wavebands. IR systems use two or three broad infrared bands discussed previously in this chapter (Harney 2013c). Figures 18 and 19 present the spectral response curves of a monochromatic and a color sensor without an IR filter. In contrast to ordinary EO/IR sensors, multispectral imagers use multiple narrow bands to capture four or more wavebands in the ultraviolet, visible, or infrared parts of the EM spectrum (Harney 2013c).

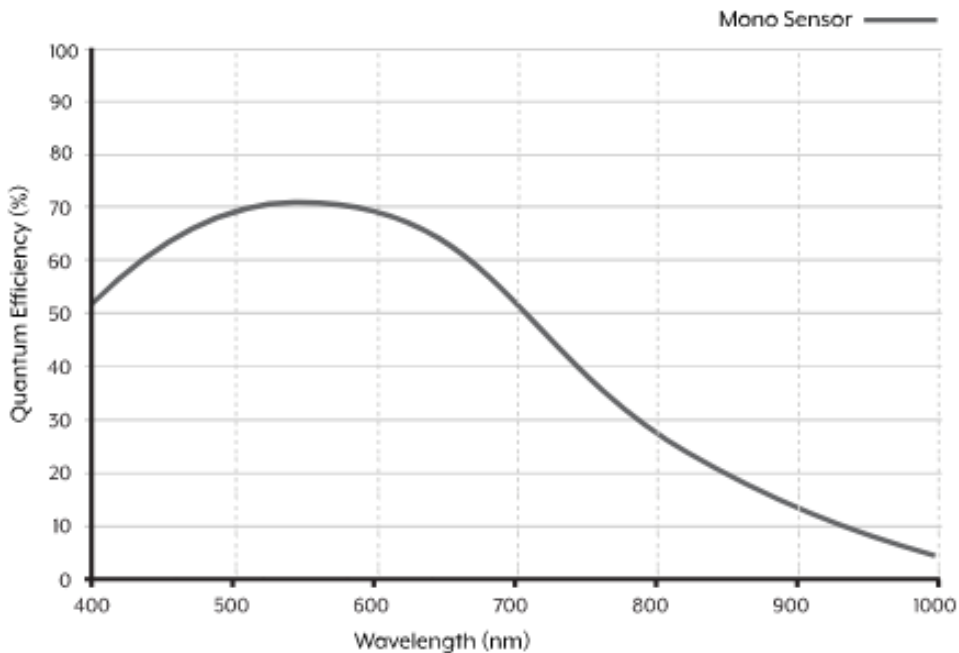


Figure 18. Spectral Response Curve of a Monochromatic Imaging Sensor.
Source: Lucid Vision Labs (2023).

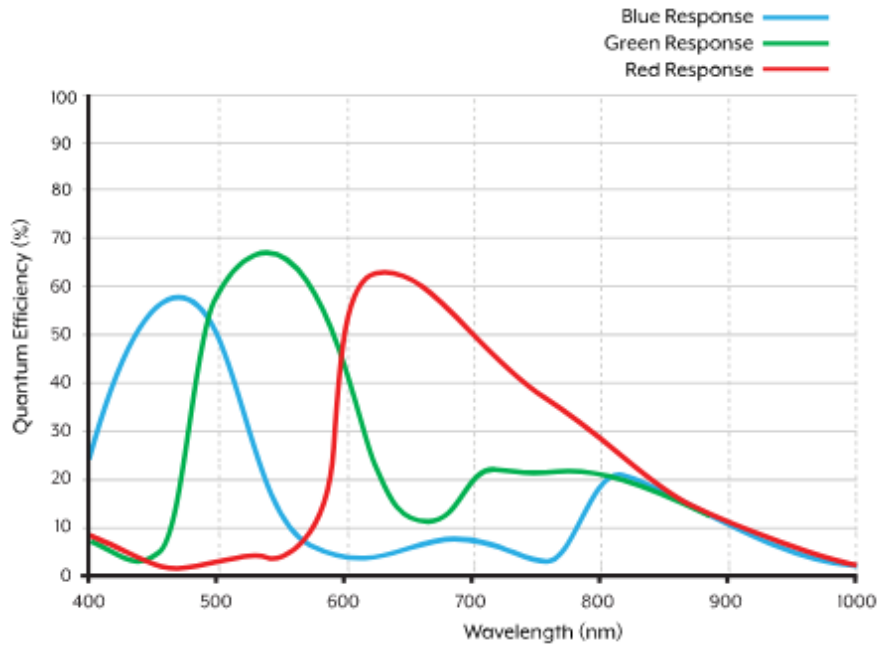


Figure 19. Spectral Response Curve of a Color Imaging Sensor. Source: Lucid Vision Labs (2023).

Harney (2013c) defines multispectral systems as systems that use four or more wavebands in ultraviolet, visible, and infrared. Systems that use more than a hundred wavebands are defined as hyperspectral. Ultraspectral has been defined for hypothetical future systems using tens of thousands of wavebands. In contrast to ordinary EO/IR sensors, the major advance of multispectral sensors is that they can “capture the underlying processes (e.g., chemical characteristics and biophysical properties) at the pixel level” (Prasad and Chanussot 2020, 1).

This advantage can be used to identify the spectral reflectance of material in each band of the systems. According to Yang, Zhao, and Chan, “the rich spectral and spatial information can be beneficial for discriminating different materials in the scene” (Yang, Zhao, and Chan 2020, 408). This capability can be used by multispectral imaging techniques, exploiting spectral data to produce imaging products not available by ordinary imaging (Skauli et al. 2014). In addition, those methods can be used to identify features of the environment or artificial objects and have and can be used in both civilian and military applications.

1. Multispectral Imaging Paradigm

Multispectral imaging can be implemented using a variety of methods. The basis for classifying those methods are the following baseline questions:

- Is each band using discrete detectors?
- Are detectors used in discrete, linear, or area arrays?
- Is a filter or mirror used?

Based on those baseline questions, the following primary methodologies of multispectral imaging can be identified:

- **Across-track scanning.** In this method, single, discrete detectors, using a scanning mirror perform an across-track scanning of the targeted area. This method is called “Whiskbroom” and uses a rotating or oscillating mirror and a prism to scan lines at right angles to the flight line (Lillesand, Kiefer, and Chipman, 2015). A visualization of this method is presented in Figure 20.a.
- **Along-track scanning.** This method uses a linear array of detectors to perform an along-track scanning of the target area. This method is also called “Pushbroom” and uses a fixed lens to capture simultaneously complete linear arrays of the target area. Filters are used to separate the different bands. A visualization of this method is presented in Figure 20.b.
- **Area arrays.** In this method, area arrays capture two-dimensional images of the target area. Multiple area arrays or filters can be used to capture different bands. A visualization of this method is presented in Figure 21.

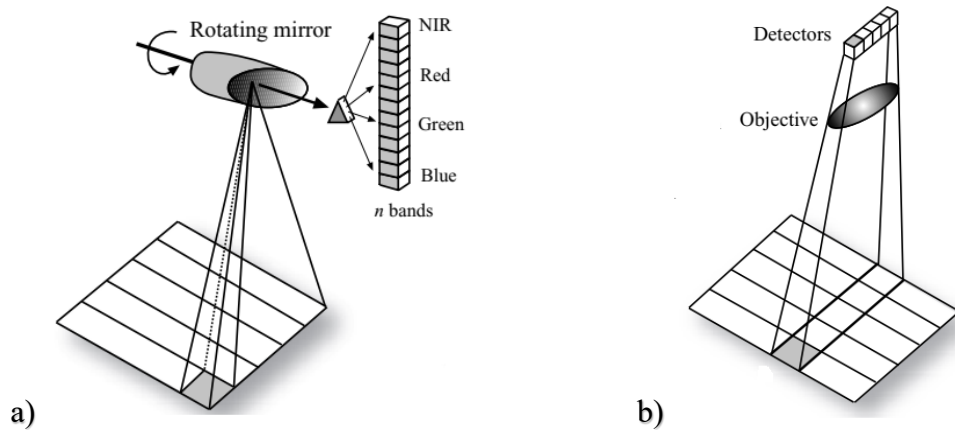


Figure 20. Across-Track (a) and Along-Track (b) Multispectral Imaging. Adapted from Jensen (2007).

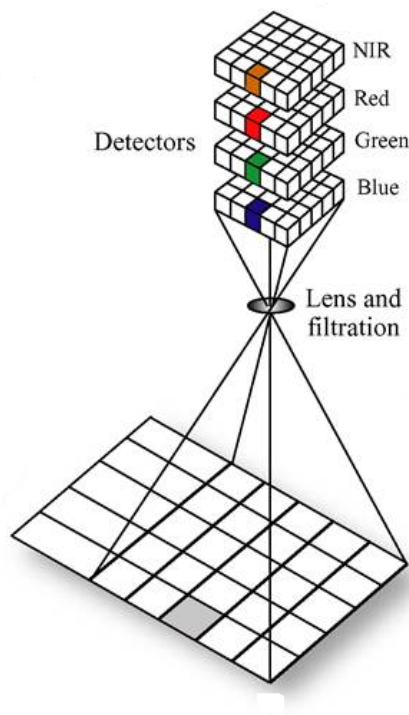


Figure 21. Area Arrays for Multispectral Imaging. Adapted from Jensen (2007).

In general, linear arrays and along-track multispectral imaging, used in the across-track method, provides several advantages against discrete detectors. First, they provide a

higher exposure time over the targeted area, enabling a higher signal-to-noise ratio. Moreover, fewer geometric errors are introduced into the data due to each sensor following a single scan line, in contrast to using mirrors to achieve the same results. Finally, eliminating a rotating mirror reduces the system's weight (Lillesand, Kiefer, and Chipman 2015). Area arrays provide the additional advantage of the simultaneous capture of a two-dimensional image, in contrast to the one-dimension capture in each exposure by linear arrays.

Multispectral and hyperspectral imaging can be an effective sensing method for civilian and military applications using small UAS. The most prominent applications are target detection and environmental mapping (Torkildsen et al. 2016). Nevertheless, spectral imaging sensors are usually large due to the necessary optics capable of extracting spectral information (Skauli et al. 2014). Designing and manufacturing such sensors, exploiting the information from reflected light in multiple bands, and integrating them into a small UAS can be challenging (Haavardsholm, Skauli, and Stahl 2020). This is the reason underlying the less common reports in the literature of applications using visible bands in contrast to multispectral applications, although lightweight multispectral sensors for UAS are being used increasingly (Laliberte et al. 2011).

Despite the difficulties in designing a multispectral sensor to be integrated into a small UAS, such a combination can result in high spatial resolutions, especially when the UAS can fly in low altitudes over the target area (Laliberte et al. 2011). When the platform using the sensor is operating in such conditions, a high area coverage rate is a key requirement to reduce flight time and operational cost (Torkildsen et al. 2016); thus, using area arrays with multiple cameras, one for each band, is the most suitable option. Multiple cameras recording one band each can increase the sensor's size and weight, making it unsuitable for use in small UAS (Haavardsholm, Skauli, and Stahl 2020). Using modern miniaturized sensor arrays, lenses, and controllers, multispectral imaging can offer more compact options than hyperspectral imaging. This is the preferable solution for such applications (Torkildsen et al. 2016).

Recent work by Hassler and Baysal-Gurel (2019) and Haavardsholm, Skauli, and Stahl (2020) has provided evidence that low-cost multispectral sensors mounted on small

UAS can provide high spatial resolution in the challenging case of wide-area mapping. Moreover, commercial solutions provided by companies like AgEagle are being extensively used in civilian applications like mapping and agriculture. Based on that evidence, using compact and low-cost COTS multispectral sensors integrated into small UAS is believed to provide significant potential for military applications.

2. Multispectral Imaging Civilian Applications

Bannari et al. note that “the spectral composition of the radiant flux emanating from the Earth’s surface provides information about the physical properties of soil, water, and vegetation features in terrestrial environments” (Bannari et al. 1995, 96) Multispectral imaging can capture that information, enabling several civilian applications, ranging from mapping to agriculture. Fabrizio identifies the following promising or well-developed fields of application that, for the purposes of this thesis, only vegetation analysis will be further discussed:

- Environmental monitoring
- Geologic mapping
- Vegetation analysis
- Atmospheric characterization and climate research
- Understanding of the structure and of the functioning of ecosystems
- Monitoring of coastal environments
- Biological and chemical detection
- Disaster assessment
- Urban growth analysis
- Gas leak detection (Fabrizio 2007, 2–1)

As mentioned before, multispectral imaging and sensing can capture the spectral reflectance of natural and man-made materials, objects, and structures based on their chemical characteristics, biophysical properties, and spectral reflectance. In the case of vegetation, pigments like chlorophyll, leaf water content, and internal scattering dominate the spectral reflectance curve of plants (Jensen 2007). Figure 22 presents a typical spectral reflectance curve of a plant.

Figure 22 shows that the highest percentage of incident EM radiation between 250 to 700 nm is absorbed due to carotenoid and chlorophyll absorption. In the red edge part

of the spectrum (700–750 nm), a steep transition from absorption to reflection is observed, due to foliar reflectance, followed by a minor transition in the SWIR part of the IR spectrum, around 1250 nm, due to liquid water absorption. We also observe that soil follows a different curve, allowing more straightforward distinction when acquiring multispectral data.

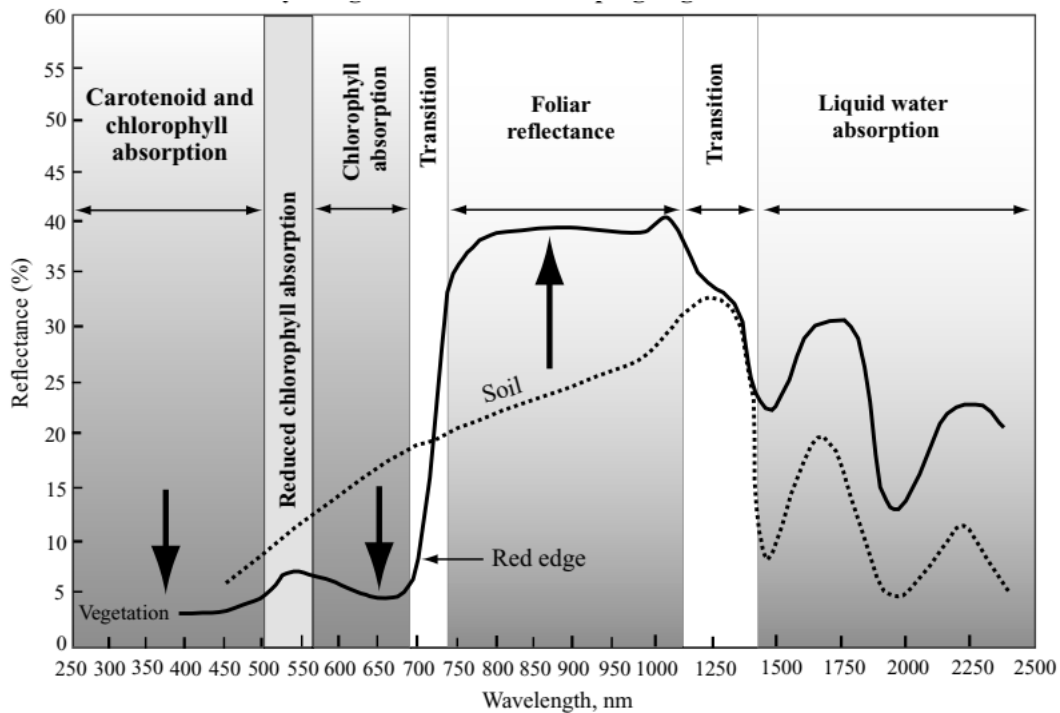


Figure 22. Typical Vegetation Spectral Reflectance Curve. Source: Jensen (2007).

The spectral reflectance curve presented in Figure 23, is unique to each plant and can be affected by several parameters, the most important being the water content of the plant. MIR is absorbed efficiently by water; thus, the higher the water content of the plant, the lower the reflectance in this part of the spectrum (Jansen 2007). Figure 23 presents such an example, showing that when a plant’s water content increases, reflectance is smaller through the spectrum. Nevertheless, due to the abovementioned increased absorption in the middle-infrared part of the spectrum, the greatest decrease is observed in the region between 1.3 and 2.5 μm .

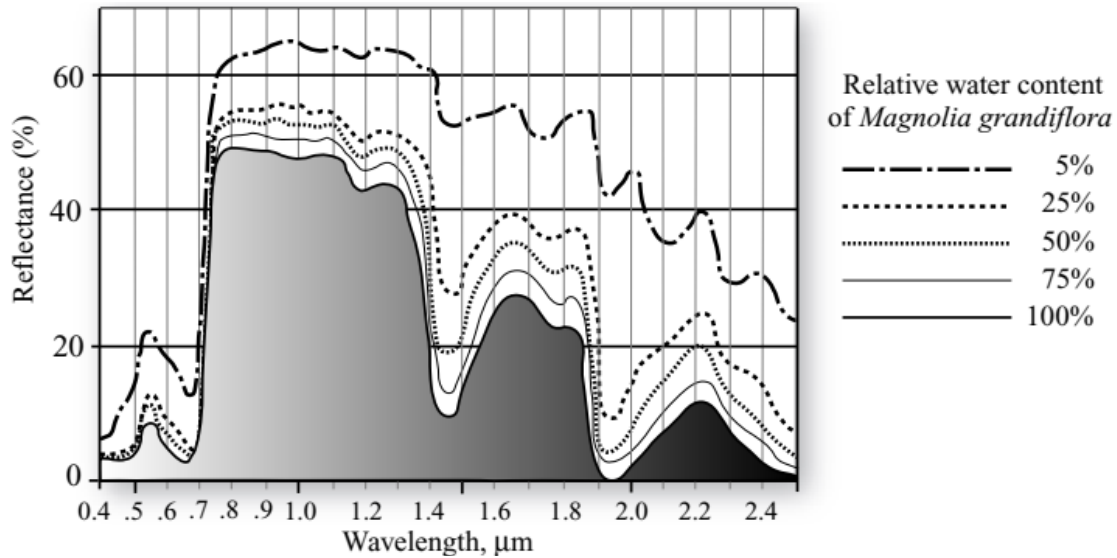


Figure 23. Reflectance Response of Leaf as a Function of Water Content.
Source: Jensen (2007).

Vegetation reflectance, as discussed above, combined with soil brightness, environmental effects, shadow, soil color, and moisture, create a complex environment; nonetheless, the spectral characteristics of this environment can be used to qualitatively and quantitatively evaluate vegetation cover. This can be achieved by using vegetation indices, which are measuring quantitatively the health and strength of vegetation by combining reflectance information from different bands, showing better sensitivity than individual bands (Bannari et al. 1995). Multispectral imaging sensors equipped on satellites, aircraft, and UAS, can gather data to calculate several vegetation indices, providing variability in the field (Hassler and Baysal-Gurel 2019).

Over the last decades, several vegetation indices have been put into practice. The first two, developed by Pearson and Miller, were simple ratios, depicting the ratio between reflectance in the red and NIR part of the spectrum. Those indices were the ratio vegetation index and the vegetation index number and are calculated using Equations (4) and (5) (Bannari et al. 1995).

$$RVI = RED / NIR \quad (4)$$

$$VIN = NIR / RED \quad (5)$$

Nowadays, the most widely used vegetation index in agriculture is the normalized difference vegetation index (NDVI). It expresses the difference between the reflectance in the NIR and Red bands, normalized by their sum. NDVI is calculated using Equation xxx and allows the measurement of crop stress as a good indicator of their health (Paredes et al. 2017). NDVI ranges between -1 and 1, with higher values indicating denser and healthier vegetation areas and lower values not healthy plants or other materials. Jensen (2007) notes that additive noise effects can influence NDVI and is sensitive to soil visible through the green leaf of the plant. This can lead to NDVI values being higher when dark soil is present. Despite its disadvantages, NDVI is widely used due to the bands used for its calculation being available in all low-cost multispectral sensors capable of being integrated into small UAS.

$$NDVI = \frac{NIR - RED}{NIR + RED} \quad (6)$$

Another method of fusing multispectral imaging and creating images that highlight vegetation is the color infrared band combination (CIR). CIR, like RGB, combines three bands to create an image. The difference between RGB and CIR is the use of narrowband multispectral bands and the combination of NIR, red, and green bands instead of red, green, and blue. Like NDVI, CIR provides the capability of identification of vegetation and estimation about their health (Jansen 2007).

Figures 24 to 28 show imaging captured during flights conducted for this thesis using multispectral sensors. The same area is presented in RGB, NIR and RED bands and calculated using the NDVI index. In Figure 26, the higher reflectance of vegetation in NIR compared to soil can be identified. In contrast, in Figure 27, the higher reflectance of soil in the red band can be observed. Figure 28 presents the calculated NDVI index for this area. It can be observed that dense and healthy-grown plants present an NDVI index close to its max value of 1, with soil presenting values around zero. Finally, Figure 25 presents the image in CIR.

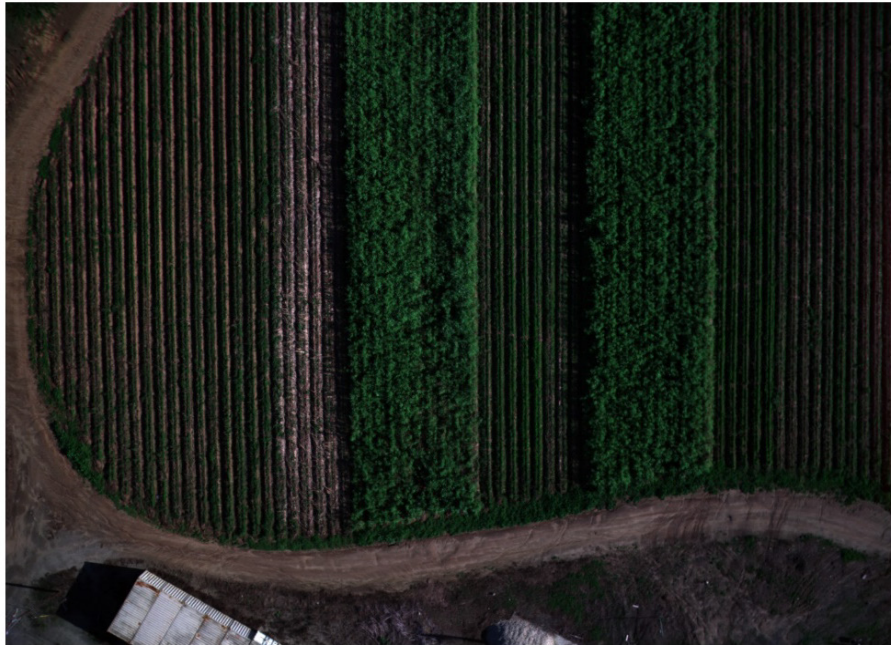


Figure 24. RGB Imaging of an Agricultural Area



Figure 25. CIR Imaging of an Agricultural Area



Figure 26. NIR Band Imaging of an Agricultural Area



Figure 27. RED Band Imaging of an Agricultural Area

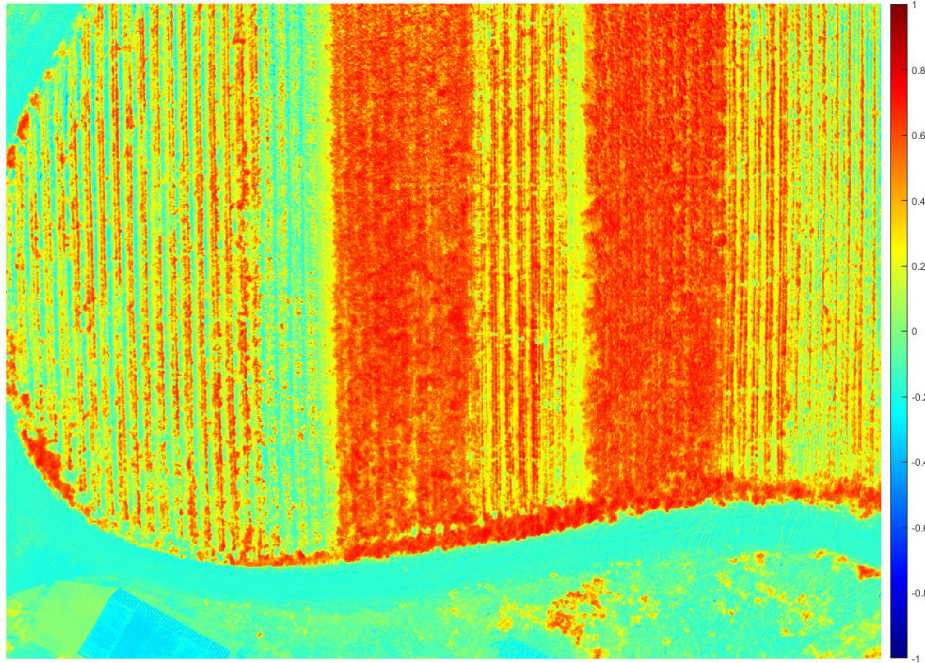


Figure 28. NDVI Imaging of an Agricultural Area

3. Multispectral Imaging Military Applications

Multispectral imaging can enable potential applications for several defense and military-related applications. Factors that can determine how practical multispectral imaging is can be identified for any application. The most common are the characteristics and capabilities of the sensor, how well the characteristics of the area under examination can be sampled, and the amount of relevant data that can be extracted using multispectral sensors (Anderson et al. 1994). Technological advances have enabled multispectral imaging to be used viably in many demanding military applications (Boucher et al. 2006). Fabrizio and Skauli et al. identify the following military applications that can be benefited from multispectral imaging:

- Gathering information about battlespace.
- Discrimination between targets and decoys.
- Defeating camouflage.
- Early warning for long range missiles and space surveillance.
- Detection of weapons of mass destruction.
- Detection of landmines.
- Monitoring of international treaty compliance.

- Automated target detection (Fabrizio 2007, 2–1)

As in the civilian sector, multispectral imaging can benefit the abovementioned applications. Using the capability to extract the unique spectral characteristics of each material, structure, or artificial object and use them to identify features and targets using methodologies like anomaly detection, signature-based detection, and band selection (Boucher et al. 2006). As mentioned above, spatial resolution is a critical requirement in multispectral imaging. Therefore, it must be at least higher than the dimensions of the smallest target that must be identified. For this reason, low-cost multispectral sensors integrated into small tactical UAS, flying in low altitudes can provide enhanced SR capabilities at the tactical level.

Two of the potential military applications that can be benefited mainly from using multispectral sensors integrated with small tactical UAS are defeating camouflage and the detection of landmines. In response to modern SR capabilities, military forces use camouflage to decrease the probability of being detected by adversaries. Additionally, landmines and improvised explosive devices (IED) cannot be easily detected due to their small size and their use methodology, which usually includes burying them in the ground. In both cases, the unique capabilities of multispectral sensors can enable methodologies to counter those threats.

Camouflage, concealment, and decoys, expressed for this thesis with the term camouflage, are defined as “the use of materials and techniques to hide, blend, disguise, decoy, or disrupt the appearance of military targets and/or their backgrounds” (DOD 2010, 1–1). Armies have been using camouflage for centuries to prevent adversaries from detecting and identifying friendly forces. Two primary methodologies of camouflage are using paints, nets, and other materials to make targets look like the environment in color and shape and hiding or blending assets with vegetation and other aspects of the environment.

Camouflage materials are designed to mimic the background environment and are widely used to reduce the probability of detection of assets passively. In recent years, modern materials have enabled the imitation of natural characteristics, providing the

capability to deceive visual and EO/IR observation (Zhou et al. 2011). One of the most widely used camouflage materials is camouflage nets. They are functional, light, cost-effective, and offer protection from observation in a wide range of wavelengths (Stein and Schleijpen 2021). Modern camouflage nets provide anti-IR and even anti-spectral capabilities, with their spectral reflectance curves designed to mimic vegetation. The spectral reflectance curve of an anti-spectral reconnaissance camouflaged net (ASRC-net) and of an anti-infrared reconnaissance camouflaged net (AIRC-net) are presented in Figure 29.

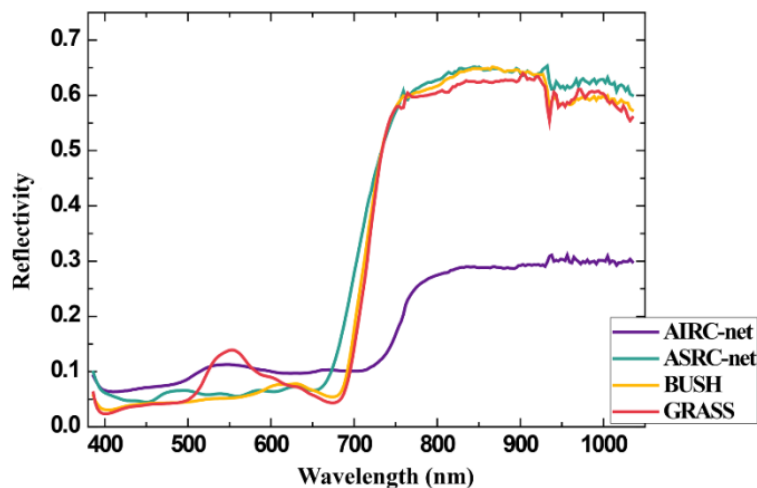


Figure 29. Camouflage Nets Spectral Reflectance Curve Compared to Vegetation. Source: Shen et al. (2021).

Landmines and IEDs are using their small size, mimicking the environment, and being buried in the ground to avoid detection from aerial SR. Several experiments have shown that multispectral imaging in the visible and NIR part of the EM spectrum can enable the detection of buried objects. This can be achieved by detecting the reflectivity variation the disturbed soil creates (Makki et al. 2017). Goldberg, Stann, and Gupta (2003) note that disturbed soil has increased emissivity in the 850 to 950 nm NIR region of the spectrum. However, due to the small size of IEDs and landmines, only sensors with high spatial resolution can achieve proper detection, making small tactical UAS necessary for this application (Makki et al. 2017).

III. EXPERIMENT SETUP

As stated in Chapter I, this thesis aims to explore if a COTS multispectral sensor integrated with a small UAS can detect the camouflaged man-made targets or battlefield anomalies. To answer this question, sufficient data must be collected and analysed. For this purpose, several experimental flights were conducted. In all flights, a COTS multispectral sensor integrated with a COTS small UAS was used to collect imagery data on a few different targets.

A. HARDWARE

This study used an AgEagle's RedEdge-P high-resolution multispectral five-band plus panchromatic sensor. The UAS used was the vertical take-off and landing (VTOL), fixed-wing Quantum System's Trinity F90+. This section provides with more specifics on both components and their integration.

1. RedEdge-P Multispectral Sensor

RedEdge-P is a low-cost five-band plus panchromatic multispectral and RGB imaging sensor. It has been designed to be integrated into small UAS and is primarily used for mapping and agricultural imaging. It is compact, and lightweight, providing adequate spatial resolution and field of view. The sensor uses a separate array for each band, with narrowband filters, coupled with a higher resolution panchromatic sensor. The sensor stores the imaging in an internal storage drive and cannot transmit images via a data link. Figures 30 and 31 present the sensor stand-alone and integrated into a quadcopter UAS.



Figure 30. RedEdge-P Multispectral Sensor. Source: AgEagle (n.d.).



Figure 31. RedEdge-P Multispectral Sensor Integrated with UAS. Source: AgEagle (n.d.).

The sensor can capture EM radiation in five narrowband bands in the visible and IR parts of the spectrum. Table 2 and Figure 32 present each band's center wavelength and bandwidth. Another critical sensor specification is the 1.6 MP and 5.1 MP resolution for each multispectral band and the panchromatic one, respectively. This resolution, combined with the 50° horizontal and 38° vertical field of view for the multispectral sensor, leads to a spatial resolution of 7.7cm per pixel at 120m altitude and 3.85cm per pixel at 60m altitude. A complete set of specifications for the sensor is presented in Tables 3 and 4.

Table 2. RedEdge-P Multispectral Bands. Source: AgEagle (2022).

Band	Center Wavelength (nm)	Bandwidth (nm)
Blue	475	32
Green	560	27
Red	668	16
Red Edge	717	12
NIR	842	57

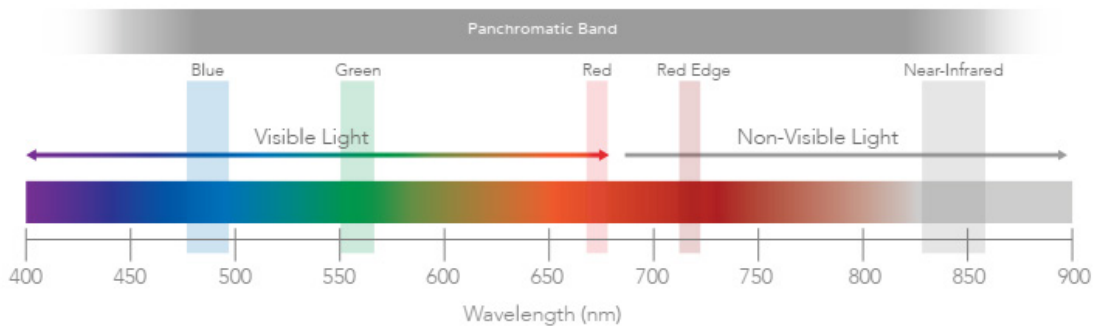


Figure 32. RedEdge-P Bands. Source: AgEagle (n.d.).

Table 3. RedEdge-P Sensors Specifications. Source: AgEagle (2022).

Specification	Multispectral	Panchromatic
Pixel size	3.45 μm	3.45 μm
Resolution	1456 x 1088 (1.58 MP per band)	2464 x 2056 (5.1MP panchromatic band)
Aspect ratio	4:3	6:5
Sensor size	6.3 mm diagonal	11.1 mm diagonal
Focal length	5.5 mm	10.3 mm
Field of view	49.6° HFOV x 38.3° VFOV	44.5° HFOV x 37.7° VFOV
Output bit depth	12-bit	12-bit
Spatial Resolution (120 m)	7.7 cm/pixel	3.98 cm/pixel
Spatial Resolution (160 m)	3.85 cm/pixel	1.99 cm/pixel for

Table 4. RedEdge-P General Specifications. Source: AgEagle (2022).

Specification	Description – Value
Weight	350 g (12.3 oz)
Dimensions	8.9 x 7.0 x 6.7 cm (3.5in x 2.8in x 2.6in)
External Power	7.0 V - 25.2 V
Storage	CFexpress card

2. Trinity F90+ UAS

Trinity F90+, presented in Figures 33 and 34, is an electrical, VTOL, fixed-wing small, and lightweight UAS, made primarily of carbon fiber and styrofoam. It is certified for integrating several sensors, ranging from EO/IR and multispectral imaging, to lidar and oblique imaging sensors. It is capable of fully autonomous, pre-planned, or semi-autonomous flights. Mission planning and monitoring are conducted using the QBase 3D

software in a portable device connected to the UAS via datalink. A complete set of specifications for the sensor is presented in Table 5.

Table 5. Trinity F90+ Specifications. Source: Quantum Systems (n.d.).

Specification	Description – Value
Max Take-off Weight	5 kg (11 lbs)
Max Flight Time	90 min
Max Range - Area	100 km–700 ha
Max Altitude	4500 m (14,763 ft)
Wind Tolerance	Up to 9 m/s (17.5 kn)
Wingspan	2.394 m (7.85 ft)
Optimal Cruise Speed	17 m/s (33 kn)
C2 Range	5–7.5 km (3.1–4.7 mil)



Figure 33. The Trinity F90+ UAS



Figure 34. The Trinity F90+ Taking Off

B. AREA OF OPERATIONS

The experimental flights for this thesis were conducted at the Naval Postgraduate School (NPS) Field Laboratory located at McMillan Airfield, inside the restricted airspace R-2504 covering the California National Guard's base at Camp Roberts. Figure 35 shows a bird's-eye view of the McMillan Airfield lab. Since airspace around NPS Field Laboratory is designated as restricted, there are fewer restrictions enabling more flexibility. Hardware available at the McMillan Airfield lab was used as test targets for gathering imaging data.



Figure 35. The NPS Field Laboratory at McMillan Airfield, Camp Roberts.
Source: Google (n.d.).

C. DATA COLLECTION PROCEDURE

The experimental flights conducted at the NPS Field Laboratory aimed to gather multispectral and panchromatic imaging of targets, presented in Figures 35 to 51 at the Appendix, under realistic daylight conditions. The flights were conducted for three consecutive days at altitude levels of 50 and 100m above ground level (AGL), with and without the use of a generic green camouflage net, and with the target in open space or under vegetation cover. Time of day, cloud coverage, and light intensity were not controlled, thus creating a variety of environmental and lighting conditions. The setup of each flight is presented in Table 6. In each flight, the following procedure was followed:

- Setting up the target
- Mission planning

- UAS and sensor pre-flight checks
- UAS taking-off
- Mission monitoring
- UAS landing
- UAS and sensor post-flight checks
- Imaging downloading
- Imaging checking
- Next flight planning using feedback from the previous sorties

Table 6. Experimental Flights Setup

Flight Number	Target	Placing	Camouflage	AGL Altitude (m)
1	Vehicle (6x6 ATV)	Open Space	No	50, 100
2			Yes	
3		Under Partial Vegetation	No	
4			Yes	
5		Under Vegetation	No	
6			Yes	
7	IED/Mine simulation	Underground	N/A	

IV. DATA ANALYSIS AND RESULTS

As discussed in Chapter I, the research questions that this thesis aims to address are the following:

- Are COTS multispectral sensors integrated with a UAS capable of detecting camouflaged man-made targets or battlefield anomalies?
- Do COTS multispectral sensors provide a better detection capability than RGB and panchromatic sensors?

To address those questions, data collected in the experimental flights conducted as described in Chapter xxx needed to be post-processed and assessed. An algorithm was developed using MATLAB programming environment to post-process the data and fuse them using suitable indexes and techniques, like the NDVI. Following the post-processing of the data, the resulting imaging was evaluated based on two criteria. The first criterion addressed the ability of the imaging to enable the detection of the targets. The second criterion examined the ability of the sensor to provide better detection compared to RGB and panchromatic imaging.

A. SELECTION OF FUSION TECHNIQUES

The purpose of the fusion techniques that were used to create images representing the area captured by the sensor was the creation of a contrast between the targets and the environment. To address this purpose, the first two fusion techniques used were the NDVI and CIR. Both those techniques, as described in Chapter II, highlight vegetation, and create a contrast to other materials in the image. This can create contrast between the target and surrounding vegetation, thus enabling its detection.

Another fusion technique that was used was developed after an examination of the data gathered in the experimental flights. Using the hyperspectral imaging toolbox, a spectral reflectance curve of the target and several materials of the environment (dirt, grass, trees, and others) was created. This curve is presented in Figure 36. We observe that the reflectance of the target (thick light blue) differs in the blue and red edge bands more than

the NIR and red used by the NDVI. Based on this observation, a new index was created, calculating the normalized difference between the reflectance in the red edge and blue bands. This index, called for the purposes of this thesis as normalized difference red edge blue (NDREB), can be calculated using Equation (7). Like NDVI, NDREB ranges between the values of -1 and 1.

$$NDREB = \frac{RE - Blue}{RE + Blue} \quad (7)$$

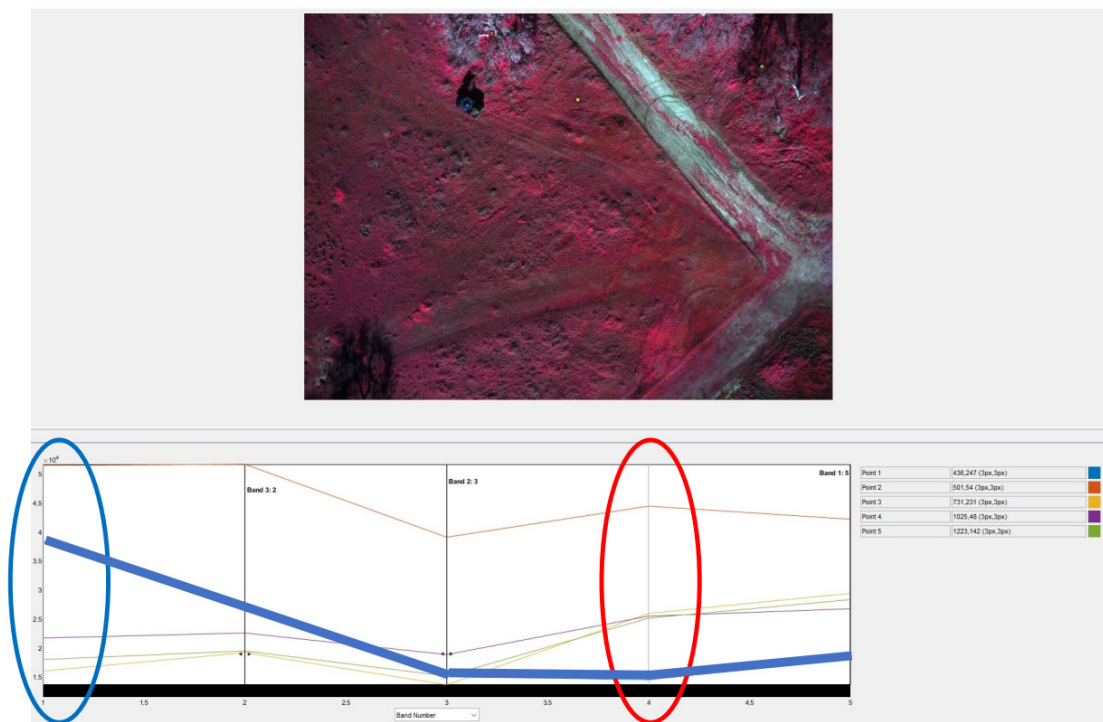


Figure 36. Spectral Reflectance Curve of Target and Environment

B. POST PROCESS ALGORITHM

As discussed in Chapter II the sensor used in the experiment creates six images for each capture. Five of those are images of the five multispectral bands, while the last one is the capture of the panchromatic sensor. The following steps were necessary to enable those images to be used by MATLAB, aiming to fuse them using indexes like NDVI:

- Import, align, and crop the images in MATLAB

- Arrange images in a hypercube
- Generation of initial fused images
- Process of initial and generation of final fused images

1. Importing, Aligning, and Cropping Images in MATLAB

The images generated by the sensor are grayscale TIF files, equivalent to a two-dimension matrix, and they are imported in MATLAB as such. Due to the individual band lenses being separated in the sensor, as presented in Figure 37, the images generated by the sensor are not aligned. When fused without proper alignment, they lead to images like the one (no camouflage and in open space), presented in Figure 38, that are unsuitable for further processing.

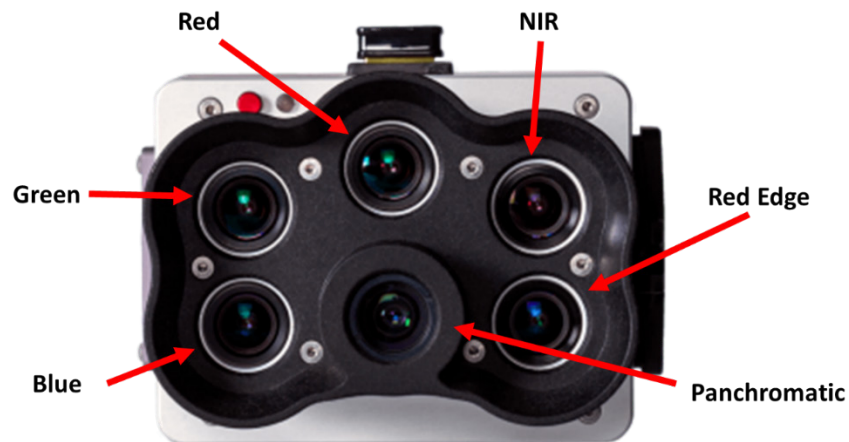


Figure 37. RedEdge-P Individual Sensors. Adapted from AgEagle (n.d.).

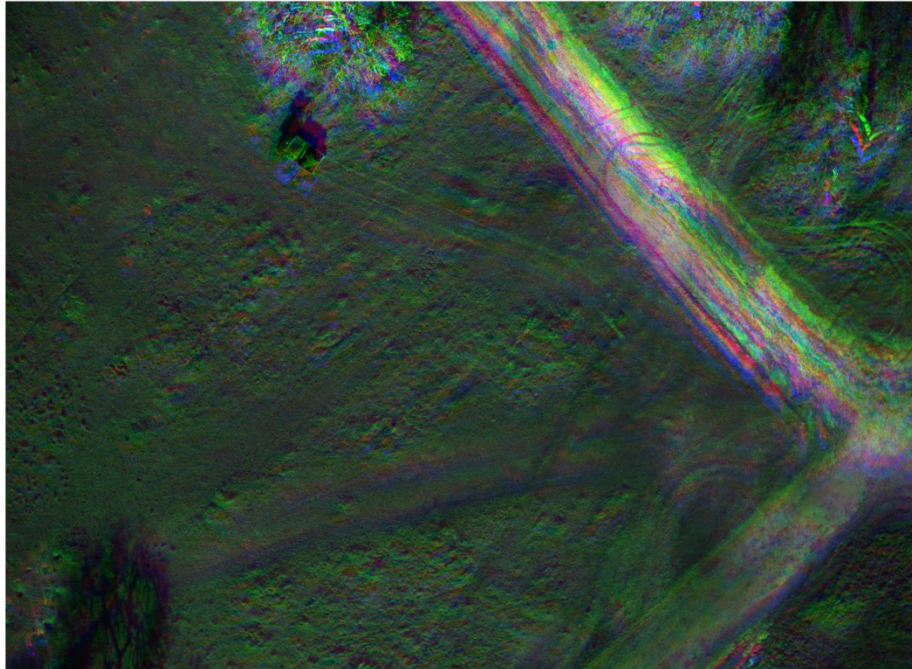


Figure 38. RGB Fusion of Unaligned Multispectral Images

A registration algorithm, built-in MATLAB as a function, was used to address the alignment issue. Image registration is an image processing technique that aligns multiple captures into one image. Image registration performs image rotation, scaling, and skew to align overlaying images like the ones generated by the sensor (MathWorks n.d.). For the purposes of this thesis, an automatic registration function using feature matching was selected. The algorithm identifies common features between two images and uses them to align one image to the other. One example of common features between the two images is presented in Figure 39.

The algorithm can align two images at each time; thus, it was used four times for each capture, with the blue, green, NIR, and red edge bands all aligned to the red band. The resulting image for the same capture as the one used in Figure 38 is presented in Figure 40. We observe that all the images are matched, but due to their original unalignment, an area in the periphery is degraded due to the use of fewer bands than needed. To address this issue, the periphery of each image was cropped. The final image created by this step of the algorithm is presented in Figure 41.

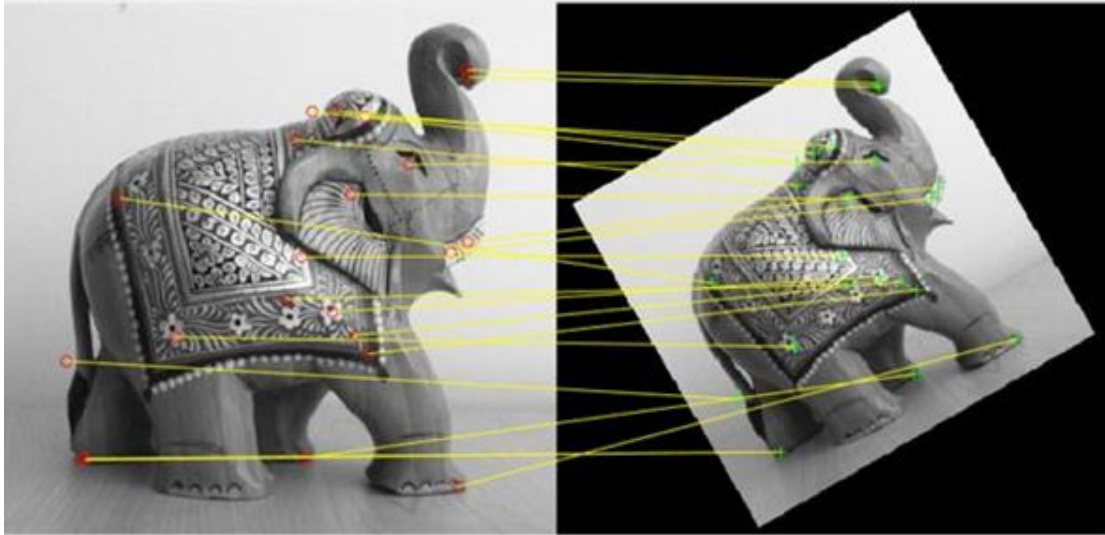


Figure 39. Example of Common Features Used in Automatic Image Registration. Source: MathWorks (n.d.).

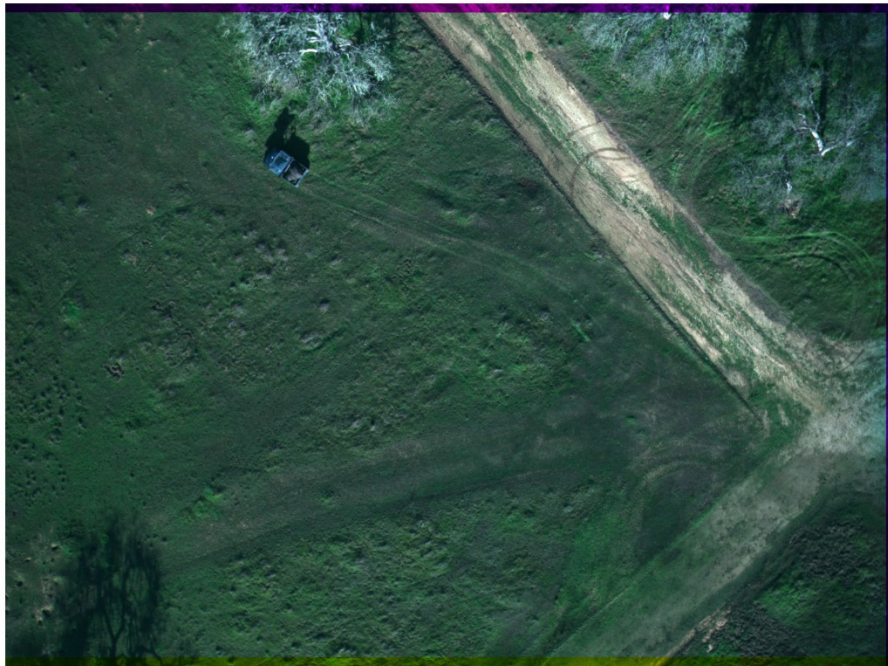


Figure 40. RGB Fusion of Aligned, Uncropped Multispectral Images



Figure 41. RGB Fusion of Aligned and Cropped Multispectral Images

The first step of the algorithm proved to be the most resource-intensive, both in computing resources and time terms. This was a direct consequence of using the registration algorithm, needing more than ten seconds to align all the images. In a real-time or near-real-time application, this delay would be unacceptable. One solution addressing this issue could be a function taking as an input the above-ground altitude in which the images were captured and providing as an output the shift that needs to be applied for each axis and in each band.

2. Arranging Images into a Hypercube

The hyperspectral imaging processing toolbox embedded in MATLAB requires the input data to be in the form of a hypercube. Hypercubes are n -dimensional analogs of squares and cubes, with squares and cubes being hypercubes with $n=2$ and $n=3$ dimensions, respectively. Moreover, hypercubes in MATLAB store metadata, the most important of them being the number of bands used and their wavelengths. In this algorithm step, the five two-dimensional arrays of each multispectral band were transformed into a three-dimensional hypercube, with each layer of the cube representing one of the bands.

3. Generating the Initial Fused Images

The next step of the algorithm was the fusion of the multispectral images using NDVI, CIR, and NDREB. Moreover, an RGB image was created to as a comparison baseline. To create the NDVI, CIR, and RGB fused images, functions provided by MATLAB's hyperspectral imaging toolbox were used. On the other hand, the generation of NDREB fused images was hardcoded in the algorithm. In the cases of the two indexes (NDVI and NDREB), MATLAB's "bone" colormap was used to represent the -1 to 1 range of values. The CIR, NDVI, and NDREB fused images of the same capture as the one in Figure 40 are presented in Figures 42 to 44, respectively.



Figure 42. CIR Fusion of Multispectral Images

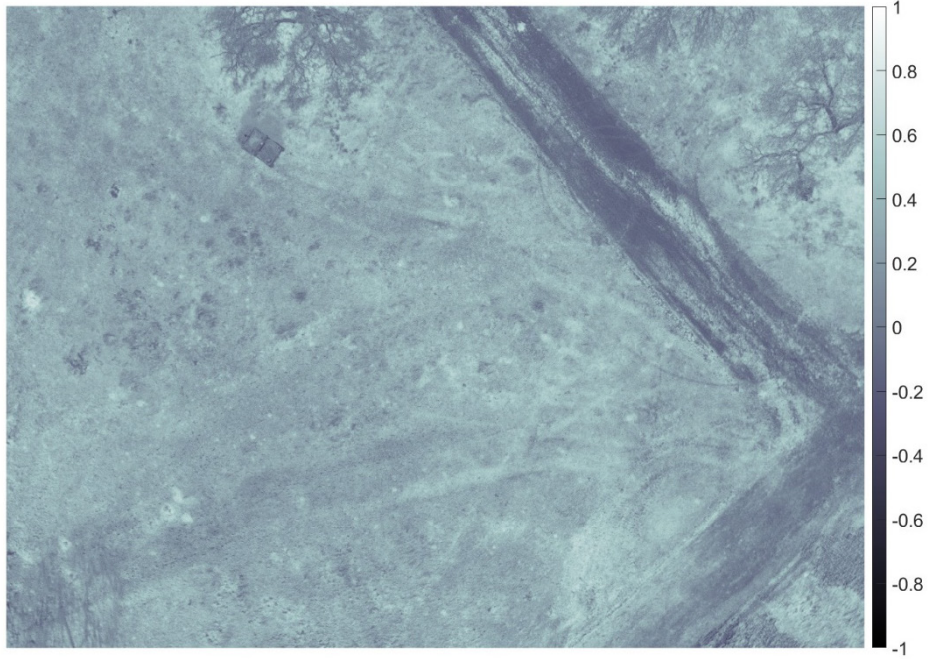


Figure 43. NDVI Fusion of Multispectral Images

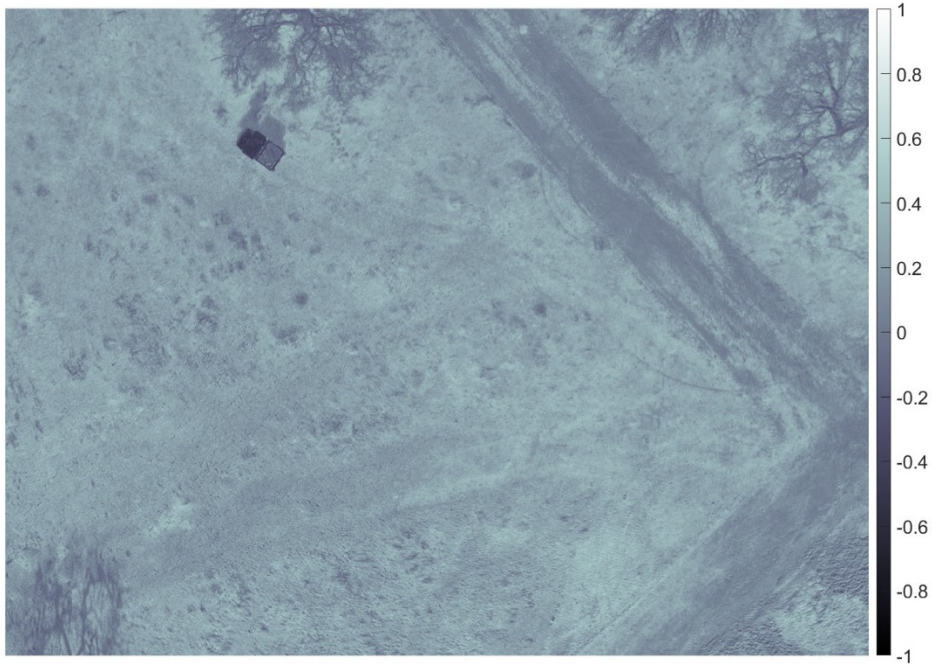


Figure 44. NDREB Fusion of Multispectral Images

4. Processing the Initial and Generating the Final Fused Images

As discussed, the NDVI and NDREB indexes range from -1 to 1. Nevertheless, the values in each image are not always using the full range of the index. Limiting the range of the colormap used to match the actual range of each image can highlight details and increase the contrast between the target and the background. Figures 45 and 46 present the same image as Figures 43 and 44, respectively, with the difference of the colormap being set to be limited to the values of each image. We observe that in both images, the contrast between the target and the environment has increased; thus, detecting the target is easier compared to the images with the full-range colormap. Contrast can be increased further by manually limiting the colormap to values closer to the ones of the target. Figures 47 and 48 present the images as Figures 45 and 46, respectively, using a manual set colormap limit. Again, we observe an increase in the contrast between the target and the environment.

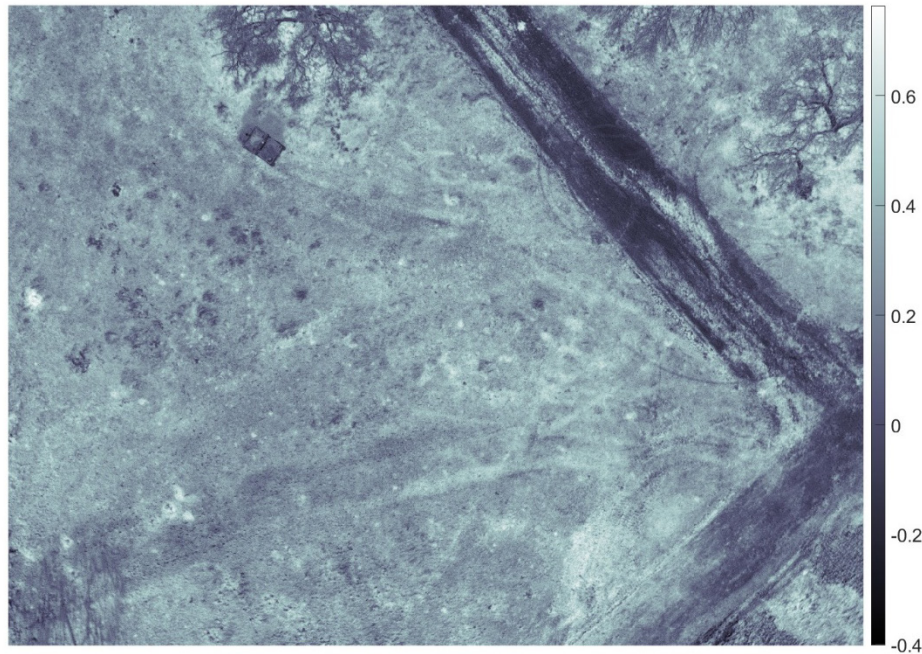


Figure 45. NDVI Fusion of Multispectral Images with Limited Colormap

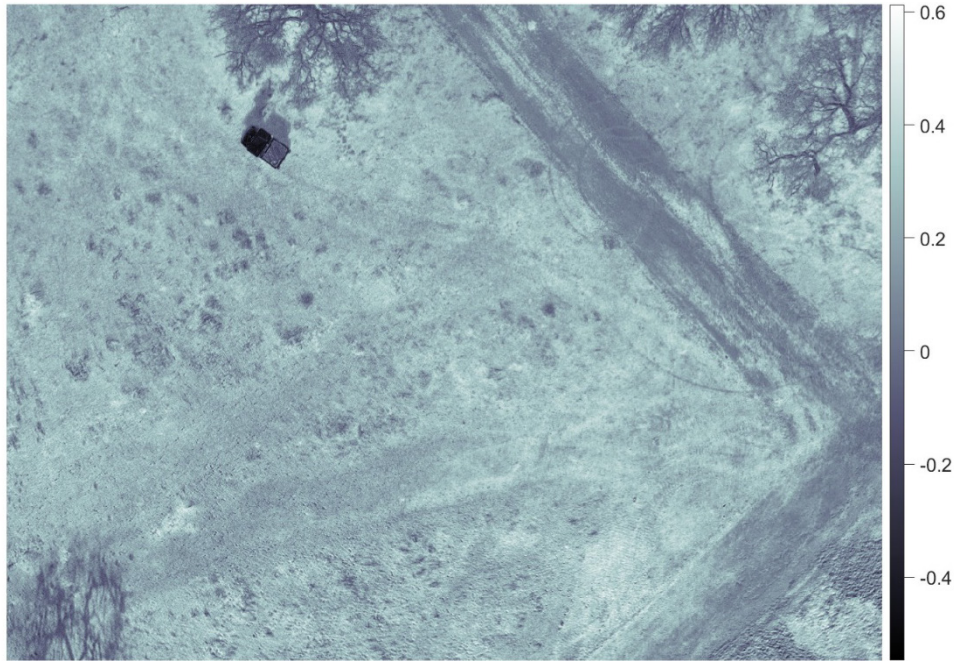


Figure 46. NDREB Fusion of Multispectral Images with Limited Colormap

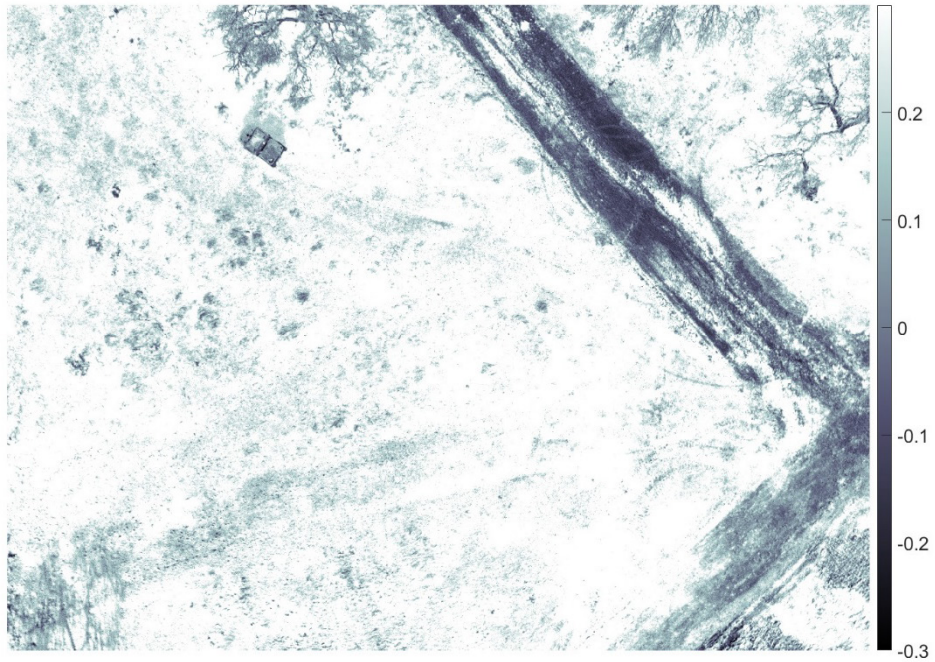


Figure 47. NDVI Fusion of Multispectral Images with Manual Limited Colormap



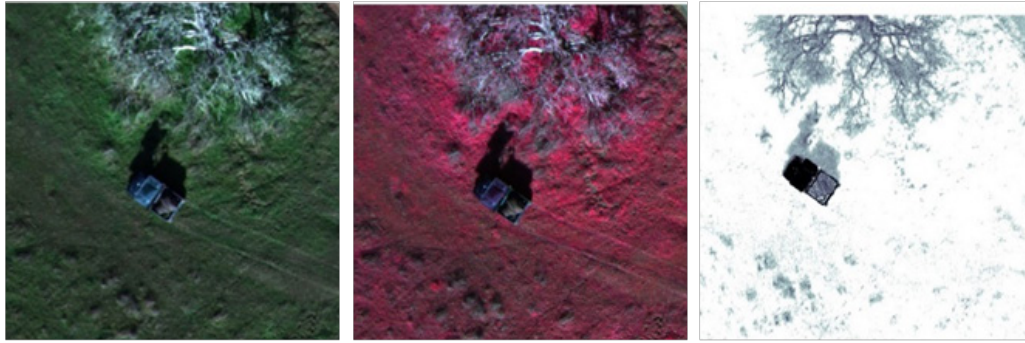
Figure 48. NDREB Fusion of Multispectral Images with Manual Limited Colormap

C. INTERPRETATION OF THE RESULTS

As described in Table 6, several scenarios of target detection were examined. The parameters that were altered between scenarios were the altitude of UAS, vegetation cover, and the usage of a camouflage net. In this subsection, the key results of each scenario are presented and discussed.

1. Detection of Target in Open Space

Images generated from captures of the target placed in an open space without a camouflage net are presented in Figures 41, 42, 47, and 48. We observe that with the use of NDREB, the contrast between the target and the environment enables the straightforward detection of the target, compared to RGB, CIR, and NDVI. Moreover, the shape of the target is easily identified. CIR also provides a high contrast; nevertheless, in contrast to NDREB, it is affected by shadows that complicate the detection and identification of the target's shape. A comparison of the target in RGB, CIR, and NDREB is presented in Figure 49.



RGB

CIR

NDREB

Figure 49. Imaging of Target in Open Space and without Camouflage, Captured from 100m AGL

When a camouflage net covers the target, NDREB again provides high contrast between the target and the environment. Nevertheless, due to the lack of shadows due to the use of a camouflage net, CIR can create a contrast comparable to NDREB. A comparison of the target in RGB, CIR, and NDREB is presented in Figure 50.



RGB

CIR

NDREB

Figure 50. Imaging of Target in Open Space and Camouflage, Captured from 100m AGL

2. Detection of Target under Partial Vegetation Cover

When the target is under partial vegetation cover and without a camouflage net, NDREB achieves a better contrast between the target and the environment and better

detects and identifies the target's shape than other methods. CIR provides better results than RGB; nevertheless, it cannot achieve the same contrast as NDREB. When the sensor's altitude is increased from 50m (Figure 51) to 100m AGL (Figure 52), the sensor's spatial resolution is adequate to detect the target when NDREB is used.

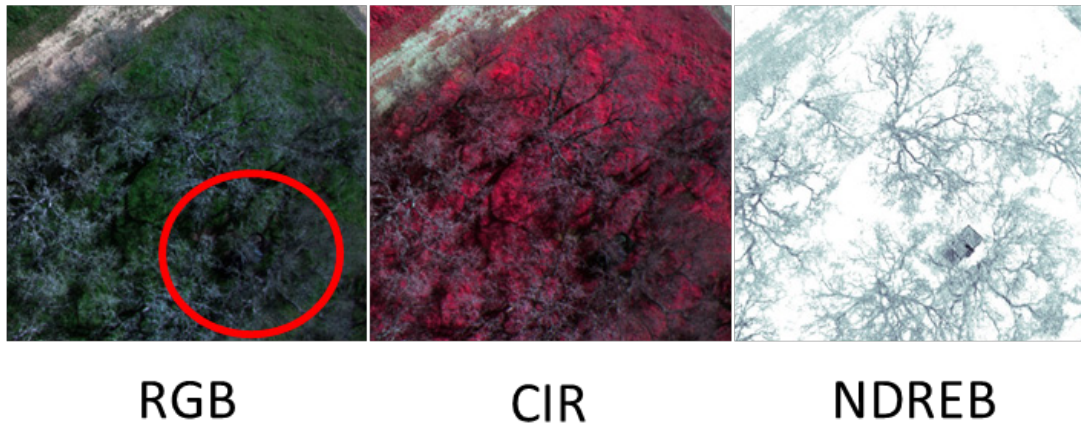


Figure 51. Imaging of Target under Partial Vegetation Cover and without Camouflage, Captured from 50m AGL

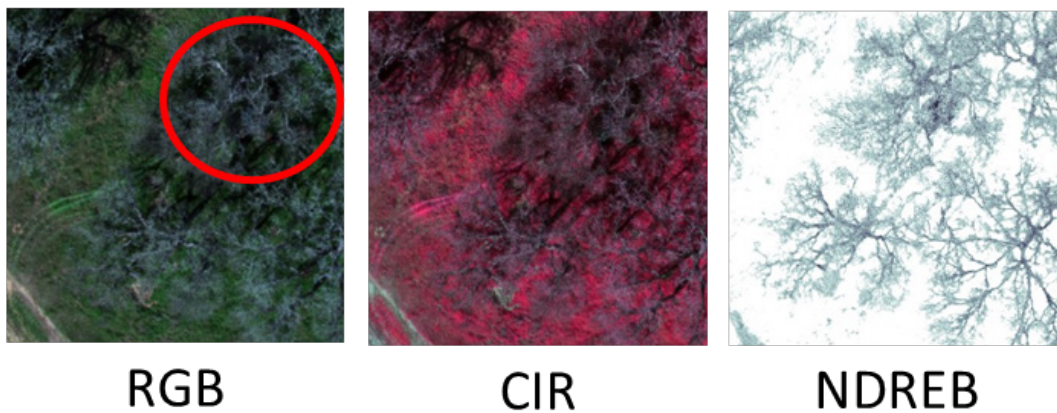


Figure 52. Imaging of Target under Partial Vegetation Cover and without Camouflage, Captured from 100m AGL

When a camouflage net covers the target, CIR provides better contrast between the target and the environment than NDREB and NDVI. The camouflage net breaks the shape of the target, thus removing the features that enable the detection of the target from the

partial vegetation cover when NDREB is used. When the sensor's altitude increases from 50m (Figure 53) to 100m AGL (Figure 54), the sensor's spatial resolution is adequate to detect the target when CIR is used.

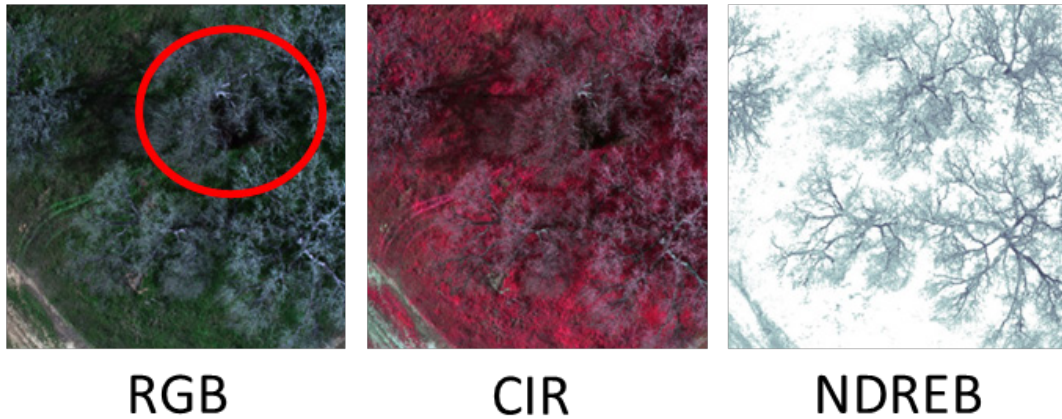


Figure 53. Imaging of Target under Partial Vegetation Cover and Camouflage, Captured from 50m AGL

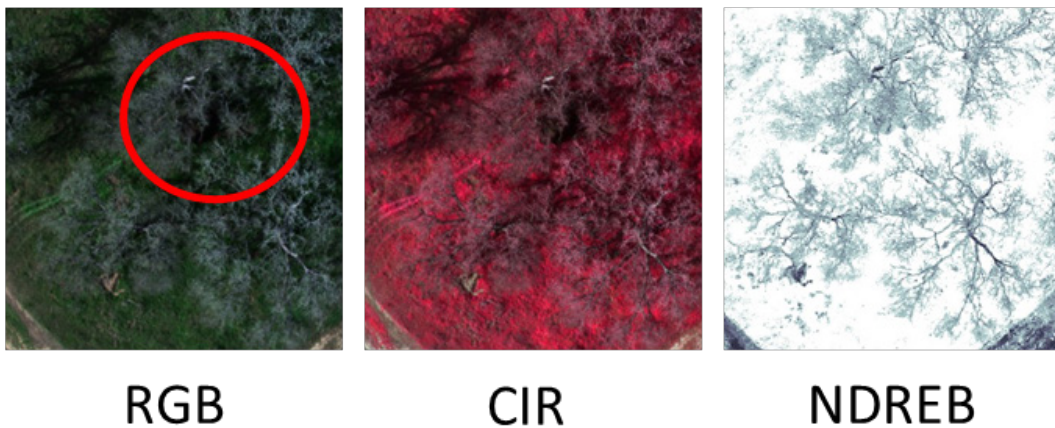


Figure 54. Imaging of Target under Partial Vegetation Cover and Camouflage, Captured from 100m AGL

3. Detection of Target under Vegetation Cover

When the target is under full vegetation cover and without a camouflage net, NDREB enables the detection of small parts of the target that may be visible. This is achieved due to the high contrast between the target and the environment, also discussed

in the previous section. In this case, CIR is not able to achieve the detection of the target. When the sensor's altitude is increased from 50m (Figure 55) to 100m AGL (Figure 56), the sensor's spatial resolution is adequate to detect the target when NDREB is used.

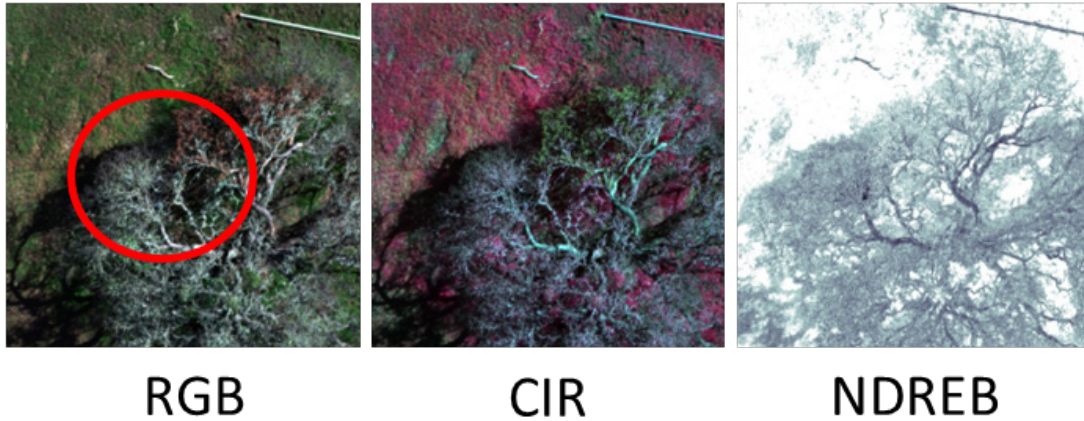


Figure 55. Imaging of Target under Vegetation Cover and without Camouflage, Captured from 50m AGL

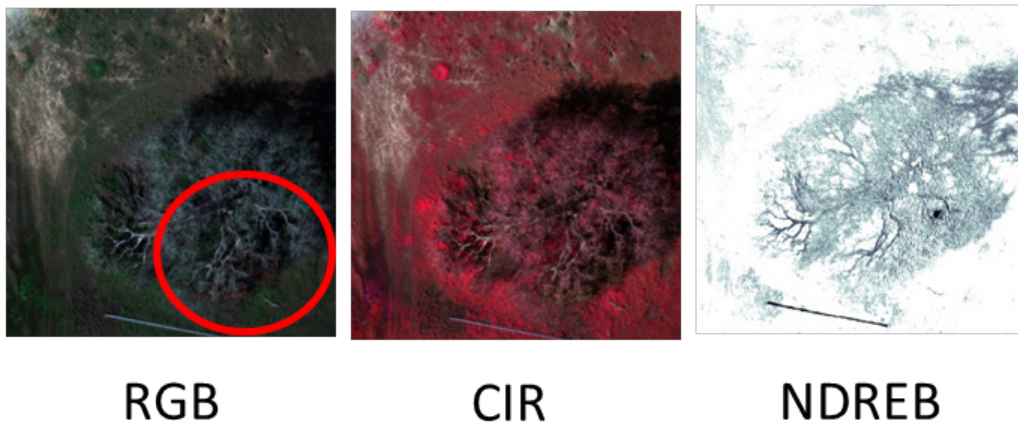


Figure 56. Imaging of Target under Vegetation Cover and without Camouflage, Captured from 100m AGL

When a camouflage net covers the target under full vegetation cover, neither NDREB nor CIR provides adequate contrast between the target and the environment to enable target detection. However, it must be noted that in the examined case presented in

Figure 57, CIR was affected by shadows degrading its ability to create contrast, thus, the results are inconclusive.

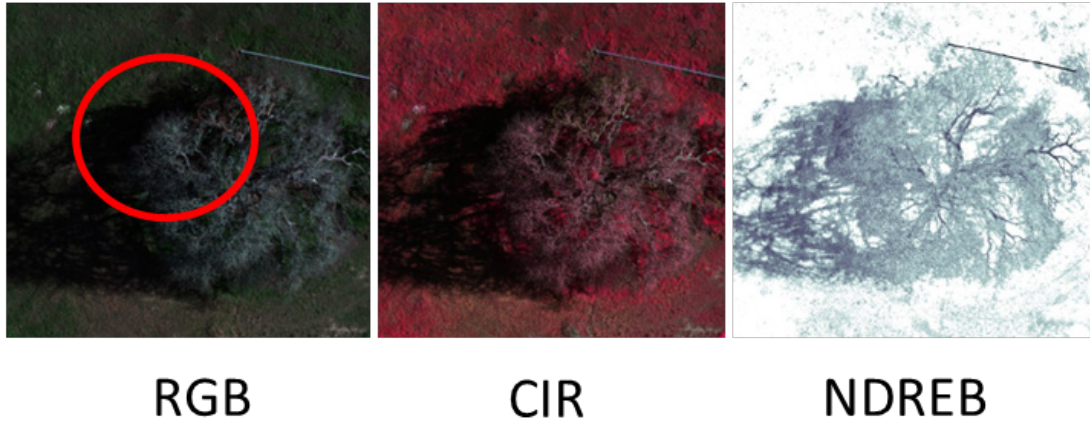
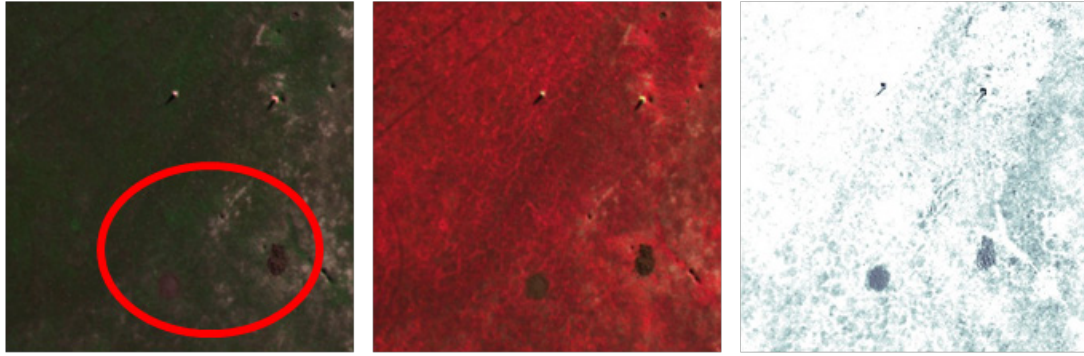


Figure 57. Imaging of Target under Vegetation Cover and Camouflage, Captured from 50m AGL

4. Detection of Landmines and IEDs

In the case of detecting freshly buried objects simulating landmines and IEDs, NDVI provided better results than NDREB, due to its ability to distinguish disturbed soil from vegetation or undisturbed soil. CIR also provided a good contrast between the targets and the environment. When the sensor's altitude is increased from 50m (Figure 58) to 100m AGL (Figure 59), the sensor's spatial resolution is adequate to detect the target when CIR and NDREB is used.

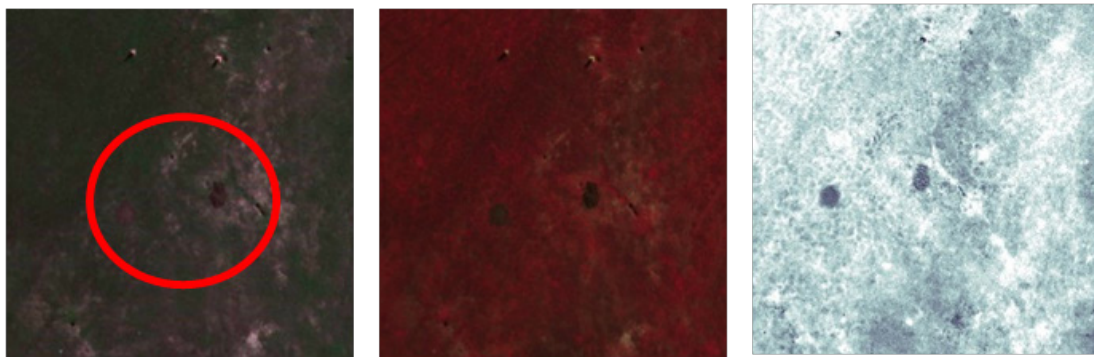


RGB

CIR

NDVI

Figure 58. Imaging of Target Captured from 50m AGL



RGB

CIR

NDVI

Figure 59. Imaging of Target Captured from 100m AGL

THIS PAGE INTENTIONALLY LEFT BLANK

V. CONCLUSIONS AND RECOMMENDATIONS

A. CONCLUSIONS

This thesis evaluated the performance of a COTS multispectral sensor in detecting camouflage targets and battlefield anomalies like mines and IEDs. After evaluating the data collected from the experimental flights conducted, using the algorithm discussed in Chapter IV, it managed to answer the two research questions set in Chapter I.

COTS multispectral sensors integrated into UAS can detect camouflaged man-made targets and battlefield anomalies. Their spatial resolution is adequate for detection, mainly when a post-process algorithm generates fused images by combining two or more bands. Moreover, COTS multispectral sensors can provide an enhanced detection capability than ordinary EO/IR. The fusion of multiple bands achieves this by generating images with enhanced contrast between the target and the environment.

The interpretation of the results, as discussed in Chapter IV, provided the following insight into the use of COTS multispectral sensors for target detection:

- The NDREB index proposed by this thesis performs better in target detection compared to the NDVI, except in the case of landmine/IEDs detection
- COTS multispectral sensors have adequate spatial resolution for detecting targets from altitudes as high as 100m AGL
- Limiting the range of indexes can enhance contrast between target and environment
- CIR is affected by shadow, degrading the capability for target detection
- NDREB performs better than CIR when the target is uncamouflaged in open spaces and equally to CIR when the target is camouflaged

- NDREB performs better than CIR when the target is uncamouflaged under partial or full vegetation cover
- CIR performs better than NDREB when the target is camouflaged under partial or full vegetation cover
- NDVI and CIR perform equally in detecting landmines and IEDs buried in the soil

In conclusion, this thesis has demonstrated that COTS multispectral sensors integrated into UAS can enhance the SR capabilities of small tactical UAS, while keeping the cost low. By doing so, it provided valuable evidence to support the development efforts of this type of UAS. Moreover, it proposed a new index suitable for post-process algorithms generating imaging products from multispectral datasets.

B. LIMITATIONS AND RECOMMENDATIONS FOR FUTURE WORK

The work done in this thesis was affected by several limitations that need to be addressed. Those are as follows:

- Flights were limited to a maximum altitude of 100m AGL
- Only one target and one camouflage net were used
- The target was placed only under one type of vegetation
- Only one type of COTS multispectral sensor was evaluated

Future work can evaluate more sensors in an expanded flight envelope and over various targets and nets. Moreover, different vegetation types need to be examined to validate the results of this thesis.

From the algorithm perspective, a real-time or near-real-time algorithm needs to be developed. The main obstacle to this direction is aligning the images generated by the individual multispectral bands. As already proposed, a function that translates AGL altitude to image shift seems to be the fastest solution. Moreover, real-time data transfer through a

datalink and post-process at the ground control station must be explored to support operational use.

From the detection efficiency perspective, images generated using the methodology tested in this thesis shall be used to train machine learning algorithms that could potentially enhance automated target detection. In addition, a significantly more extensive set of images shall be collected to enable the proposed training process.

THIS PAGE INTENTIONALLY LEFT BLANK

APPENDIX. TARGETS CONFIGURATION



Figure 60. Target at Flight No. 1.



Figure 61. Target at Flight No. 2.



Figure 62. Target at Flight No. 3.



Figure 63. Target at Flight No. 4.



Figure 64. Target at Flight No. 5.



Figure 65. Target at Flight No. 6.



Figure 66. Targets at Flight No. 7.

LIST OF REFERENCES

- AgEagle. 2022. "RedEdge-P Integration Guide." November 08, 2022.
<https://support.micasense.com/hc/en-us/articles/4410824602903-RedEdge-P-Integration-Guide>.
- AgEagle. n.d. "RedEdge-P." Accessed April 30, 2023. <https://ageagle.com/drone-sensors/rededge-p-high-res-multispectral-camera/>.
- Anderson, R., W. Malila, R. Maxwell, and L. Reed. 1994. *Military Utility of Multispectral and Hyperspectral Sensors*. 246890-3-F. Ann Arbor, MI: Environmental Research Institute of Michigan. <https://apps.dtic.mil/sti/citations/ADA325724>
- Austin, Reg. 2010. *Unmanned Aircraft Systems: UAVS Design, Development and Deployment*. West Sussex, UK: Wiley.
- Bannari, A., D. Morin, F. Bonn, and A. R. Huete. 1995. "A Review of Vegetation Indices." *Remote Sensing Reviews* 13 (1–2): 95–120. <https://doi.org/10.1080/02757259509532298>.
- Blom, John David. 2010. "Unmanned Aerial Systems: A Historical Perspective." Occasional Paper, Combat Studies Institute Press.
<https://www.armyupress.army.mil/Portals/7/combats-studies-institute/csi-books/OP37.pdf>
- Briottet, X., Y. Boucher, A. Dimmeler, A. Malaplate, A. Cini, M. Diani, H. Bekman et al. 2006. "Military Applications of Hyperspectral Imagery." In *Defense and Security Symposium*, 62390B. <https://doi.org/10.1117/12.672030>.
- Center for Strategic and Budgetary Assessments. 2013. *Thinking About the U.S. Military's Next Generation UAS Force*. HQ0034-09-D-3007-0013.
https://www.esd.whs.mil/Portals/54/Documents/FOID/Reading%20Room/Litigation_Release/Litigation%20Release%20-%20Thinking%20About%20the%20U.S.%20Military%27s%20Next%20Generation%20UAS%20Force%20Final%20Report%20%20201309.pdf
- Defense Science Board. 2016. *Summer Study on Autonomy*. Washington, DC: Department of Defense. <https://apps.dtic.mil/sti/citations/AD1017790>
- Department of the Army. 2010. *Camouflage, Concealment, and Decoys*. FM 20-3. Washington, DC: Department of the Army. <https://irp.fas.org/doddir/army/attp3-34-39.pdf>

- Fabrizio, Vagni. 2007. *Survey of Hyperspectral and Multispectral Imaging Technologies*. RTO Technical Report RTO-TR-SET-065-P3. NATO Research and Technology Organization. <https://apps.dtic.mil/sti/pdfs/ADA473675.pdf>
- Glade, David. 2010. "Unmanned Aerial Vehicles: Implications for Military Operations." Occasional Paper, Center for Strategy and Technology of Air War College. <https://apps.dtic.mil/sti/pdfs/ADA425476.pdf>
- Goldberg, A.C., B. Stann, and N. Gupta. 2003. "Multispectral, Hyperspectral, and Three-Dimensional Imaging Research at the U.S. Army Research Laboratory." In *Proceedings of The Sixth International Conference of Information Fusion, 2003* 499–506. <https://doi.org/10.1109/ICIF.2003.177488>.
- Google. n.d. "Google Maps." Accessed April 30, 2023. <https://www.google.com/maps/@36.5946007,-121.890413,15z>.
- Gupta, Suraj G., Mangesh Ghonge, and Pradip M. Jawandhiya. 2013. "Review of Unmanned Aircraft System (UAS)." *International Journal of Advanced Research in Computer Engineering & Technology* 2 (4) (April):1646-58 <https://doi.org/10.2139/ssrn.3451039>.
- Haavardsholm, Trym Vegard, Torbjorn Skauli, and Annette Stahl. 2020. "Multimodal Multispectral Imaging System for Small UAVs." *IEEE Robotics and Automation Letters* 5 (2): 1039–46. <https://doi.org/10.1109/LRA.2020.2967301>.
- Harbaugh, Matthew. 2018. "Unmanned Aerial Systems (UAS) for Intelligence, Surveillance, and Reconnaissance (ISR)." DSIAC-2018-0849. Defense Systems Information Analysis Center. <https://dsiac.org/wp-content/uploads/2018/05/UNMANNED-AERIAL-SYSTEMS-UAS-FOR-INTELLIGENCE-SURVEILLANCE-AND-RECONNAISSANCE-ISR.pdf>
- Harney, Robert. 2013c. *Combat Systems Engineering, Volume 1: Sensors Signals and Functions*. Monterey: Naval Postgraduate School.
- Harney, Robert. 2013a. *Combat Systems Engineering, Volume 2: Sensor Technologies*. Monterey: Naval Postgraduate School.
- Harney, Robert. 2013b. *Combat Systems Engineering, Volume 5: Command and Control Elements*. Monterey: Naval Postgraduate School.
- Hassler, Samuel C., and Fulya Baysal-Gurel. 2019. "Unmanned Aircraft System (UAS) Technology and Applications in Agriculture." *Agronomy* 9 (10): 618. <https://doi.org/10.3390/agronomy9100618>.
- Hoehn, John, Kalley Sayler, and Michael DeVine. 2022. *Unmanned Aircraft Systems: Roles, Missions, and Future Concepts*. R47188. Washington, DC: Congressional Research Service. <https://sgp.fas.org/crs/weapons/R47188.pdf>

- Huete, A. R. 2004. "Remote Sensing for Environmental Monitoring." In *Environmental Monitoring and Characterization*, edited by Janick F. Artiola, Ian L. Pepper, and Mark L. Brusseau, 183–206. Burlington: Academic Press. <https://doi.org/10.1016/B978-012064477-3/50013-8>.
- Jensen, John R. 2007. *Remote Sensing of the Environment: An Earth Resource Perspective*. 2nd ed. Essex, UK: Prentice Hall.
- . 2015. *Introductory Digital Image Processing: A Remote Sensing Perspective*. 4th ed. Essex, UK: Pearson Hall.
- Joint Chiefs of Staff. 2010. *Dictionary of Military and Associated Terms*. JP 1-02. Washington, DC: Joint Chiefs of Staff. https://irp.fas.org/doddir/dod/jp1_02.pdf.
- . 2019. *Joint Air Operations*. JP 3-30. Washington, DC: Joint Chiefs of Staff. https://www.jcs.mil/Portals/36/Documents/Doctrine/pubs/jp3_30.pdf.
- . 2022. *Joint Intelligence*. JP 2-0. Washington, DC: Joint Chiefs of Staff. <https://www.jcs.mil/Doctrine/Joint-Doctrine-Pubs/2-0-Intelligence-Series/>.
- Laliberte, Andrea S., Mark A. Goforth, Caitriana M. Steele, and Albert Rango. 2011. "Multispectral Remote Sensing from Unmanned Aircraft: Image Processing Workflows and Applications for Rangeland Environments." *Remote Sensing* 3 (11): 2529–51. <https://doi.org/10.3390/rs3112529>.
- Lillesand, Thomas, Ralph Kiefer, and Jonathan Chipman. 2015. *Remote Sensing and Image Interpretation*. 7th ed. West Sussex, UK: Wiley.
- Lucid Vision Labs. n.d. "Understanding the Digital Image Sensor." *Lucid Vision Labs Tech Brief* (blog). Accessed April 20, 2023. <https://thinklucid.com/tech-briefs/understanding-digital-image-sensors/>.
- Makki, Ihab, Rafic Younes, Clovis Francis, Tiziano Bianchi, and Massimo Zucchetti. 2017. "A Survey of Landmine Detection Using Hyperspectral Imaging." *ISPRS Journal of Photogrammetry and Remote Sensing* 124 (February): 40–53. <https://doi.org/10.1016/j.isprsjprs.2016.12.009>.
- Mathworks. n.d. "Hyperspectral Image Processing." Accessed April 29, 2023. <https://www.mathworks.com/help/images/hyperspectral-image-processing.html>
- Mikkelsen, Alexander, and Gorm K. Selj. 2021. "Spectral Properties of Multilayered Oak Leaves and a Camouflage Net: Experimental Measurements and Mathematical Modelling." In *Target and Background Signatures VII*, edited by Karin U. Stein and Ric Schleijsen, 2. <https://doi.org/10.1117/12.2597968>.

- Moreno-Martínez, Álvaro, María Piles, Jordi Muñoz-Marí, Manuel Campos-Taberner, Jose E. Adsuara, Anna Mateo, Adrián Perez-Suay, Francisco Javier García-Haro, and Gustau Camps-Valls. 2020. “Machine Learning Methods for Spatial and Temporal Parameter Estimation.” In *Hyperspectral Image Analysis*, edited by Saurabh Prasad and Jocelyn Chanussot, 5–35. Cham: Springer International Publishing. https://doi.org/10.1007/978-3-030-38617-7_2.
- NATO. 2023. “Joint Intelligence, Surveillance and Reconnaissance.” April 11, 2023. https://www.nato.int/cps/en/natohq/topics_111830.htm.
- Office of the Assistant Secretary of Defense for Acquisition. 2017. *Unmanned Systems Integrated Roadmap 2017–2042*. Washington, DC: Department of Defense. <https://apps.dtic.mil/sti/pdfs/AD1059546.pdf>
- Office of the Secretary of Defense. 2005. *Unmanned Aircraft Systems Roadmap 2005–2030*. Washington, DC: Department of Defense. https://irp.fas.org/program/collect/uav_roadmap2005.pdf
- Office of the Secretary of Defense. 2007. *Unmanned Systems Roadmap: 2007–2032*. Washington, DC: Department of Defense. https://www.globalsecurity.org/intell/library/reports/2007/dod-unmanned-systems-roadmap_2007-2032.pdf
- Paredes, Juan, Jessenia Gonzalez, Carlos Saito, and Andres Flores. 2017. “Multispectral Imaging System with UAV Integration Capabilities for Crop Analysis.” In 2017 *IEEE International Symposium of Geoscience and Remote Sensing* 1–4. <https://doi.org/10.1109/GRSS-CHILE.2017.7996009>.
- Prasad, Saurabh, and Jocelyn Chanussot. 2020. “Introduction.” In *Hyperspectral Image Analysis*, edited by Saurabh Prasad and Jocelyn Chanussot, 1–4. Cham: Springer International Publishing. https://doi.org/10.1007/978-3-030-38617-7_1.
- Quantum Systems. n.d. “Discover Trinity F90+.” Accessed January 23, 2023. <https://quantum-systems.com/trinity-f90/>.
- Schott, John R. 2007. *Remote Sensing: The Image Chain Approach*. 2nd ed. New York: Oxford University Press.
- Selj, G. K., and M. Söderblom. 2015. “Discriminating between Camouflaged Targets by Their Time of Detection by a Human-Based Observer Assessment Method.” In *SPIE Security + Defence*, 965305. <https://doi.org/10.1117/12.2195150>.
- Shen, Ying, Jie Li, Wenfu Lin, Liqiong Chen, Feng Huang, and Shu Wang. 2021. “Camouflaged Target Detection Based on Snapshot Multispectral Imaging.” *Remote Sensing* 13 (19): 3949. <https://doi.org/10.3390/rs13193949>.

- Skauli, T., and I. Kåsen. 2005. “The Effect of Spatial Resolution on Hyperspectral Target Detection Performance.” In *European Symposium on Optics and Photonics for Defense and Security*, 59870V. <https://doi.org/10.1117/12.631313>.
- Skauli, Torbjørn, Hans Erling Torkildsen, Stephane Nicolas, Thomas Opsahl, Trym Haavardsholm, Ingebjørg Kåsen, and Atle Rognmo. 2014. “Compact Camera for Multispectral and Conventional Imaging Based on Patterned Filters.” *Applied Optics* 53 (13): C64. <https://doi.org/10.1364/AO.53.000C64>.
- Skauli, Torbjørn, Trym V. Haavardsholm, Ingebjørg Kåsen, Gunnar Arisholm, Amela Kavara, Thomas Olsvik Opsahl, and Atle Skaugen. 2010. “An Airborne Real-Time Hyperspectral Target Detection System.” In *SPIE Defense, Security, and Sensing*, 76950A. <https://doi.org/10.1117/12.850443>.
- Torkildsen, Hans Erling, Trym Haavardsholm, Thomas Opsahl, Urmila Datta, Atle Skaugen, and Torbjørn Skauli. 2016. “Compact Multispectral Multi-Camera Imaging System for Small UAVs.” In *Algorithms and Technologies for Multispectral, Hyperspectral, and Ultraspectral Imagery*, 98401U. <https://doi.org/10.1117/12.2224495>.
- U.S. Army UAS Center of Excellence. 2010. “*Eyes of the Army*”: U.S. Army Roadmap for Unmanned Aircraft Systems 2010–2035. Fort Rucker, Alabama: U.S. Army.
- Wikipedia. n.d.a. “AeroVironment RQ-11 Raven.” Accessed April 18, 2023. https://en.wikipedia.org/w/index.php?title=AeroVironment_RQ-11_Raven&oldid=1148952338.
- Wikipedia. n.d.b. “KH-11 KENNEN.” Accessed January 15, 2023. https://en.wikipedia.org/w/index.php?title=KH-11_KENNEN&oldid=1149638594.
- Wikipedia. n.d.c. “General Atomics MQ-1 Predator.” Accessed January 15, 2023. https://en.wikipedia.org/wiki/General_Atomics_MQ-1_Predator
- Yang, Jingxiang, Yong-Qiang Zhao, and Jonathan Cheung-Wai Chan. 2020. “Hyperspectral–Multispectral Image Fusion Enhancement Based on Deep Learning.” In *Hyperspectral Image Analysis*, edited by Saurabh Prasad and Jocelyn Chanussot, 407–33. Cham: Springer International Publishing. https://doi.org/10.1007/978-3-030-38617-7_14.
- Zhou, Pu-cheng, Feng Wang, Hong-kun Zhang, and Mo-gen Xue. 2011. “Camouflaged Target Detection Based on Visible and near Infrared Polarimetric Imagery Fusion.” In *International Symposium on Photoelectronic Detection and Imaging 2011*, 81940Y. <https://doi.org/10.1117/12.899590>.

THIS PAGE INTENTIONALLY LEFT BLANK

INITIAL DISTRIBUTION LIST

1. Defense Technical Information Center
Ft. Belvoir, Virginia
2. Dudley Knox Library
Naval Postgraduate School
Monterey, California



DUDLEY KNOX LIBRARY

NAVAL POSTGRADUATE SCHOOL

WWW.NPS.EDU

WHERE SCIENCE MEETS THE ART OF WARFARE